Emergent Materials (2023) 6:453–481
https://doi.org/10.1007/s42247-023-00485-0

REVIEW

A review of soft magnetic properties of mechanically alloyed amorphous and nanocrystalline powders

Alican Yakin[1] · Tuncay Simsek[2] · Baris Avar[3] · Telem Simsek[4] · Arun K. Chattopadhyay[5]

Received: 2 January 2023 / Accepted: 13 March 2023 / Published online: 11 April 2023

Abstract
The development of soft magnetic materials is fundamentally important for improving operational efficiencies of the ever-growing field of power electronics, electrical motors, and generators. It requires to meet the challenges of constantly changing fields of modern areas of applications starting from spaceships to day-to-day electronics. Many new materials with soft magnetic properties, viz. ferrous alloys, soft ferrites, amorphous and nanocrystalline magnetic alloys, have been continuously evolving since the inception of electromagnetic induction. The main drive for the continuous improvements of soft magnetic materials is primarily to enhance energy efficiency, to reduce size and weight, and to boost the power of high-frequency power electronics and electrical machines of high rotational speed. Despite some predicaments, the amorphous and nanocrystalline soft magnetic materials have become a field of major research interest since their invention four decades ago. It has been observed that the amorphous and nanocrystalline alloys exhibit better magnetic properties than the conventional soft magnetic alloys. This group of materials is produced adapting various production techniques. In this review, amorphous, nanocrystalline, and high entropy alloys (HEA) are discussed as soft magnetic materials and their electromagnetic properties are assessed. However, this review will particularly focus on the mechanically alloyed amorphous, nanocrystalline, and HEA soft magnetic materials. The soft magnetic alloys of interest for this review are grouped on the basis of Fe, Co, Ni, and FeCoNi. Furthermore, the effect of MA parameters and subsequent annealing processes on the magnetic properties is also assessed. This review brings forth a great promise in the field of soft-core magnets for high-end applications.

Keywords Amorphous materials · Nanocrystalline alloys · High entropy alloys · Mechanical alloying · Soft magnetic properties

1 Introduction

A realization about the importance of soft magnetic materials actually initiated by Michael Faraday since he discovered electromagnetic induction with iron, a single-element system, in 1831. Since then, it has become a growing interest with the industrial growth and modernization, and there has been a continuous search for the new materials with improved properties for various fields of applications. As a preamble to this review, it is important to remember that in the beginning use of iron as a core material happened to be an obvious choice because of its highest room-temperature magnetization value compared to any other elements known and also for its large magnetic permeability. Nevertheless, despite iron being a simple and single element-based soft magnetic material, it has opened opportunities to search for new materials for further improvements in magnetic properties. Besides improvement in mechanical properties, annealing iron also decreases coercivity due to stress relief and makes iron more effective for inductive applications. In an inquest for new materials that can perform even better than iron, initially scientists and engineers started to find ways to boost the properties of soft iron. Since the invention of silicon steel (3% Si and 97% Fe) in 1900 as a first step toward the improvement, there had been a long period of lull until 1933 when grain-oriented silicon steel was invented for enhanced magnetic permeability [1]. Because of its low cost, high magnetization, and high permeability values, it is not a surprise that silicon steel has been holding a major share of the global soft magnet market [2] for a long time. Moreover, due to their excellent corrosion resistance, relatively low production costs, and remarkable soft magnetic properties,

✉ Tuncay Simsek
tuncaysimsek@kku.edu.tr

Extended author information available on the last page of the article

ferrosilicon and other ferrous alloys happen to be the subject of more extensive studies until today [3, 4]. A surge in the application of amorphous alloys as a new class of magnetic materials began with the invention of Duwez et al in 1967 [5]. Their findings with iron-cobalt-based amorphous alloys of greatly reduced coercivity continued with a big leap to find newer applications. The incorporation of some supportive metals in amorphous alloys to enable the formation of ultrafine crystallites was first observed by Yoshizawa et al [6]. Annealed Co-Fe amorphous alloy with added Nb and Cu metals produced small and closely spaced nanocrystallites of 10 nm in size within the amorphous phase of the Co-Fe alloy [6]. This discovery marked as the dawn of the new era of nanocrystalline soft magnetic alloys.

Demand for this type of materials started growing with changing application scenarios since then. The properties of the group of very common materials could not meet all preferred properties needed as the field of application expanded. Therefore, in order to meet these needs, scientists developed materials that could exhibit superior properties than the existing materials for similar applications. Amorphous alloys exhibit good soft magnetic properties aside from high strength, corrosion resistance, and wear resistance compared to other material groups [4, 7, 8]. Considering the usage areas of soft magnetic materials, it is seen that this group of materials is used in many areas from transformers for the distribution of electrical energy to the devices used in our day-to-day life encompassing the field of applications starting from agriculture to entertainment, and healthcare to space and warfare [9, 10]. In general, power transformers used in the distribution of electrical energy suffer from intense energy losses. Using transformer-core materials of improved soft magnetic properties, e.g., the materials of high saturation magnetization (M_s), low coercivity (H_c), and high permeability (μ) can minimize eddy current losses [10, 11]. In amorphous alloys, the formation of isolated transition metal crystallites helps to reduce such losses in comparison to the conventional magnetic materials such as iron, Si-steels, and soft ferrites. Although conventional soft magnetic materials are still very common to find, the applications of amorphous and nanocrystalline alloys, bulk metallic glasses, and high entropy alloys (HEA) are very new in that respect [8, 9]. Nevertheless, they are gaining more and more market acceptance in modern high-frequency power electronics and electrical equipment. Despite their higher initial cost, these materials of comparable M_s are favored over the conventional magnetic materials due to their low losses. Considering the lifetime usage of the electrical equipment and power electronics, the use of advanced amorphous and nanocrystalline alloys is more economic after all. This has also been predicted by Coey that the amorphous/nanocrystalline alloys with soft magnetic properties are soon to be considered as prolific alternatives to many material groups in the near future due to their superior properties [12]. While comparing the soft magnetic properties of amorphous alloys vis-à-vis other traditional alloys, viz. Fe-Ni, Fe-Co, Ni-Co, and Fe-Si, it is seen that the competitive strength of amorphous alloys with respect to saturation magnetization (M_s) is quite high [9, 12, 13]. In magnetic alloys, the interface between the separated magnetic domains, so to speak domain wall, undergoes transitions between different magnetic moments with an angular displacement of 90° or 180°. It is a gradual reorientation of individual moments across a finite distance, a correlation length. The anisotropy of magnetic alloy defines the wall thickness, which generally extends across around 100–150 atoms. The anisotropy is lowest when the individual magnetic moments are aligned with the crystal lattice axes thus reducing the width of the domain wall. Magnetic properties of the amorphous alloys are predominantly determined by the spontaneous magnetization and internal stresses. The structures of the magnetic domains and identifying domain walls are dependent on long-range and short-range stresses. It is known that the movement of magnetic wall fields or domain walls in the amorphous phase is easier than the crystalline materials. Besides, the reduced energy required to rotate the magnetic domains in amorphous alloys, their magnetic anisotropy is also reduced. It has been investigated that the reason for such low anisotropy is due to the random arrangement of the atoms in amorphous materials. They are less resistant to magnetization than the crystalline materials. This means that the energy loss is lower in amorphous materials compared to the crystalline materials [9].

Amorphous nanocrystalline materials can be produced at an industrial scale by several methods of synthesis. The production methods adopted for industrial manufacture are melt-spinning, copper mold-casting, arc-melting, suction-casting, centrifugal-casting, and mechanical alloying (MA) methods etc. [8, 14, 15]. Among all methods, MA method is the most preferred one particularly because of its high potential for synthesizing materials for widespread applications. MA provides a various stable and metastable materials [16]. The metastable materials produced by MA cover mainly but not limited to supersaturated solid solutions, intermediate phases, quasicrystalline phases, amorphous alloys, and high-entropy alloys. The MA involves repeated cold welding, fracturing, and rewelding of powder particles [17]. During the MA process, the particle size of the alloying powder is controlled by the continuous fracturing and welding events. The particle sizes decrease progressively with milling time. With prolonged milling, particle size decreased to the nanometer levels. In MA, by selecting an appropriate milling parameter such as elemental powder quantity, milling media, ball to powder ratio, milling speed, and periods, the process of synthesis of the desired material can be well controlled. MA's advantages feature especially its relatively low

equipment cost, its simple technique to control the process, and particularly its ability to synthesize both equilibrium and non-equilibrium materials at room temperature [7, 18, 19]. In addition, an added process of annealing can further enable production of amorphous-nanocrystalline alloys with improved mechanical, magnetic, and thermal properties [20, 21]. This study reviews only the soft magnetic amorphous-nanocrystalline and high entropy alloys those are produced by MA method. Furthermore, the effect of MA method on the magnetic properties of such alloys is also reviewed.

1.1 History of magnetic amorphous/nanocrystalline alloys

With the brief delineation on the history of soft magnetic materials as described above, it is also important to know the historical background of amorphous and nanocrystalline alloys and their developments over the HEAs as competitive materials in the softcore magnet sector. This review mainly concentrates on the amorphous/nanocrystalline magnetic materials that have been advancing with a great rapidity due to their superior performance as far as M_s and core loss values are concerned. With the advancement of technology and industrial growth, demands for high-performance magnetic materials started looming large. Soon, it was realized that the conventional magnetic materials were insufficient to meet the market needs. Although Duwez and his co-workers started publishing in 1960 on a new class of materials called metallic glass with the existence of nanocrystallinity within the amorphous matrix [22, 23], the existence of amorphous magnetic material was not known until their serendipitous finding in 1967 (Fig. 1) [20]

During the development of planar flow casting of Fe-P-C alloy, Duwez adopted a rapid solidification (RS) process at a cooling rate of 10^6 C/s. By virtue of ultra-fast cooling of the alloy, it led to the formation of an amorphous alloy of Fe-P-C. It was also noticed that the magnetic properties of the amorphous ferrous alloys were much better than the conventional ones. After this discovery, amorphous alloys became the center of attention among the scientific community and subsequently it became the subject of many studies later on [23, 24]. However, generating an understanding of the superior magnetic properties of the amorphous alloys began with the study of Alben et al. in 1978 [25]. In their model of random anisotropy in the amorphous phase, the presence of the crystalline phase is either negligible, or they may be present in the form of micro-crystallites embedded within the amorphous matrix. Because of that reason, the magneto-crystalline anisotropy becomes very negligible; conversely, the magnetic correlation length becomes longer than the structural correlation length in amorphous ferromagnetic materials. That is why the higher values of M_s and μ are the characteristics of an amorphous magnetic material. Later on, this random anisotropy model was further applied to the nanocrystalline materials by Herzer [26]. By studying the grain structure of the nanocrystalline ferromagnets, Herzer found that the reason for smaller effective anisotropy was due to the fact that the ferromagnetic nanocrystals were

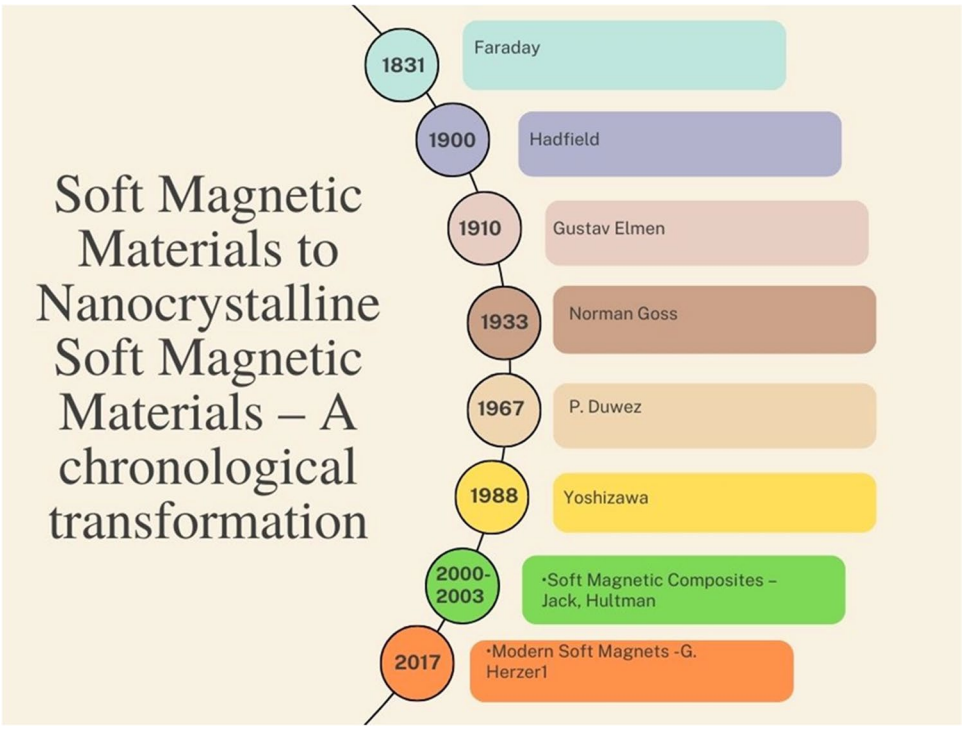

Fig. 1 Soft magnetic materials to nanocrystalline soft magnetic materials — a chronological transformation [20]

magnetically interconnected with the ferromagnetic amorphous matrix. The pioneering work of Yoshizawa et al. on the synthesis of Fe-Cu-Nb-Si-B amorphous-nanocrystalline alloy was first reported back in 1988 [6]. As reported by Yoshizawa et al., an optimized composition allowed partial devitrification of the metallic glass during controlled heat treatment. This process resulted in a nanocrystalline soft magnetic material that consisted of 10-nm diameter ferromagnetic nanograins embedded in an amorphous matrix (i.e., glass-ceramic) [6]. Because of relatively high polarization (P) for both amorphous and nanocrystalline alloys in comparison to their crystalline and thin lamination forms, eddy current losses in these materials were very low and that allowed them to operate more efficiently. Later on, developing strip-shaped amorphous alloys were succeeded. Afterwards three fundamental criteria for the formation of bulk metallic glasses (BMG) were proposed by Inoue et al [24]. Nanocrystalline alloys were obtained by applying processes under certain conditions to obtain thermodynamically metastable amorphous phases of the alloys. The subsequent nanocrystalline phases of the alloys can be achieved by subjecting the amorphous phase to certain controlled process conditions for controlling the grain sizes within nanometer scale [9, 11]. There are alloys that are completely nanocrystalline from the beginning of their formation, like Ni-P alloys produced by the electrodeposition method [27].

1.2 Soft magnetic properties of amorphous/nanocrystalline alloys

Soft magnets play a key role in power generation, distribution and conversion, magnetic sensors, magnetic recording, security, and smart composite technologies. As per the Market Analysis Report from Grandview Research "Soft Magnetic Material Market Size, Share & Trends Analysis Report by Application (Motors, Transformers, Alternators), By Product (Electrical Steel, Soft Ferrite, Permalloys), And Segment Forecasts, 2020–2027," the global soft magnetic material market of approximate size of USD 20 billion in 2020 was expected to grow at a compound annual growth rate (CAGR) of 3.9% from 2020 to 2027 [28]. With the growing demands for power distribution and advanced motors for various applications particularly for medical applications, the market growth rate may propel further highlighting the importance of the understanding and fabrication of advanced materials with superior magnetic and mechanical properties and cost-effective method of production. The efficiency of soft magnetic materials can be identified by narrow magnetic hysteresis implying that they can be easily magnetized or demagnetized with a small amount of energy. These materials generally have high induction and permeability for some applications and high operating temperatures with good mechanical properties. General considerations for good soft magnets are low coercivity (H_c), minimum core losses, high saturation magnetization (M_s), high permeability, high Curie temperature, and high resistivity [29].

The traditional crystalline soft magnetic materials are iron or iron-based alloys. Pure iron is a significantly soft material with high permeability and low coercivity. However, its low resistivity causes eddy current losses when subjected to the high flux density. Among iron-based alloys, Fe-Ni alloys are the most commonly used due to their higher permeability, saturation magnetization, and resistivity. In Fe-Ni class of alloys, the most notable one is Ni-rich Fe-Ni (20:80) permalloy for its very high magnetic permeability making it very useful as a magnetic core material for electrical and electronic equipment. They are also used for magnetic shielding to block magnetic fields. A major problem of Fe-Ni alloys is their high eddy current losses, which were resolved by the discovery of soft ferrites owing to their high electrical resistivity (10–108 μohm m). Particularly insulating ferrites are attractive for high-frequency applications such as power supplies, microwave devices, and antennas. Because of their low cost and efficient working at high frequencies, soft ferrites become more popular in the market. However, their relatively low M_s is a major hindrance to their wider applications.

Conventionally in microstructured magnets, coercivity decreases with increasing grain size following the inverse relationship between grain size (D) and coercivity (H_c) as $H_c \, \alpha \, D^{-1}$ [30]. The underlying physics of this behavior can be simply explained by the decrease in the grain boundaries which act as pinning centers for the domain walls. However, H_c follows a D^6 dependence for nanostructured magnets with very small grain sizes, which is a result of averaging out of the magnetocrystalline anisotropy [31]. This property allows to engineer nanocrystalline magnets of lower H_c by controlling the grain size [32]. In amorphous soft magnets, as they do not have any long-range atomic order, nor do they even present magnetocrystalline anisotropy and grain boundaries, the coercivity is lowered further. Nevertheless, amorphous soft magnets are known to present lower saturation magnetization when compared to polycrystalline metal alloys and nanocrystalline alloys. Amorphous metals usually fabricated by rapid solidification techniques in the form of ribbons. Most investigated amorphous alloys are (Fe,Co,Ni)x(B,Si)100−x (x =70–85, at.%) where structure contains metalloids such as B and Si. Moreover, addition of elements such as Nb, Mo, Zr to Fe-based alloys leads the glass formation that stabilizes the amorphous structure [33]. For example, 1977 Becker et al. produced amorphous $Fe_{80}B_{20}$ binary alloy ribbons with a high M_s of 1.61 T [34]. When 10% Fe is replaced by Co, M_s of 1.65 T is obtained in the cost of high price [35]. The saturation magnetization of the amorphous

alloys is usually lower than crystalline alloys due to the non-magnetic Si and B content. In 2008, Fe-Si-B-based amorphous alloys with good soft properties of 1.65 T M_s, high permeability, and extremely low core loss have been discovered and patented under the trade name METGLAS [29]. More recently, Fe-rich Fe–Si–B–P(-C) amorphous ribbons were successfully produced and high saturation magnetization of 1.7 T and low coercivity below 5 A/m was achieved in combination with good mechanical properties [36]. In 2017, high-cost P-free $(Fe_{0.8}Co_{0.2})_{85}B_14Si_1$ with increased B and decreased Si content was reported. The amorphous alloy present very high M_s of 1.92 T and low H_c of 2 A/m, which can be a very alternative to commercial Fe-Si alloys, especially for high power applications [37].

Nanocrystalline structured magnets can be produced by using the metastable amorphous phase by controlling the experimental processes. For example, the addition of an annealing step with Nd and Cu elements, isolated nanometer-sized transition metal crystallites are known to form within the amorphous matrix. In Fig. 2, XRD patterns, TEM images, selected area diffraction patterns (SAED), and grain size distributions of $Fe_{73.5}Si_{15.5}B_7Nb_3Cu_1$ ribbons treated by free annealing (FA) and hot isostatic pressing (HIP) are shown. Results show that annealing and HIP processes lead to formation of bcc α-Fe (Si) nanocrystallites embedded in amorphous matrix [38]. For that reason, these types of magnets are named amorphous/nanocrystalline soft magnets and their eddy current losses are substantially reduced when compared to soft amorphous alloys. As can be seen in the figure, the variations of their structural properties in the nanoscale giving the flexibility to tune their magnetic properties make this class of magnets attractive. For example, FINEMENT® with outstanding properties is described as TL$(1-x)$(TE, M, NM)x where TL denotes a late ferromagnetic transition metal, TE an early transition metal, M is metalloid, and NM is a noble metal, and x is usually lower than 0.2 which means that the magnet contains as much Co, Ni, or Fe as possible. The early transition metals such as Zr, Nb, Hf, and Ta along with metalloids (B, P, Si, etc.) promote the glass formation and the addition of noble metals (Cu, Ag, Au, etc.) helps the nucleation of the ferromagnetic nanocrystalline phase. The most famous example is Fe-Cu-Nb-Si-B alloy which is produced by annealing of amorphous melt-spun ribbons. Yoshizawa et al. [6] showed that excellent soft magnetic properties were obtained by the addition of two elements Cu and Nb to Fe-Si-B, which have the effect of increasing the crystallization temperature and retarding the grain growth. Thus, the alloy has an ultra-fine grain structure composed of bcc-Fe solid solution with a diameter of about 10 nm. The fine distribution of crystalline grains within the amorphous matrix was explained to cause low magnetic anisotropy and magnetostriction leading to excellent soft magnetic properties including low core losses, saturation induction of about 1.2 T, and high permeability of 100000 at 1 kHz. Moreover, the coercivity of the alloys decreases to values comparable to those of very large crystals, which can be explained using the random anisotropy model [39]. Another type of nanocrystalline/amorphous soft magnets is Fe-TM-B-based NANOPERM alloys with larger concentrations of Fe within 83–89%. The alloys have higher saturation inductions between 1.6 and 1.7 T and permeabilities up to 15000 at 1 kHz which makes them effective material for electrical power distribution transformers [40]. Consequently, several studies reported nanocrystalline (Fe, Co)–M–B–Cu (where M=Zr, Hf, Nb, etc.) alloys are patented under the trade name HITPERM. It is composed of nanocrystalline α'-FeCo grains with a B2 structure resulting in significantly improve high-temperature magnetic properties when compared to FINEMENT and NANOPERM. The reason for the good soft magnetic properties of all these amorphous/nanocrystalline materials can basically originate from grains that are much smaller than the exchange coherence length. The ferromagnetic exchange correlation length is expressed as follows:

$$L_{ex} = \sqrt{\frac{A}{K_1}} \tag{1}$$

where A denotes the exchange stiffness and constant and K_1 is the magnetocrystalline anisotropy. When the crystallite size is smaller than $L_{ex,}$ each grain behaves as a single domain, and the domain wall effect weakens. For that reason, coercivity can be calculated by using the random anisotropy model as follows [41]:

$$H_c = \frac{P_c D^6 K_1^4}{\mu_0 M_s A^3} \tag{2}$$

where P_c is a constant, and D is the crystallite size. The linear dependence of H_c to the sixth power of D means that even a small reduction in crystallite size of amorphous/nanocrystalline materials can reduce the coercivity significantly. Thus, the soft magnetic character can be improved by tailoring the nanoscale structure of amorphous/nanocrystalline alloys, and properties such as reduced coercivity and increased ac permeability can be obtained as compared with conventional alloys. For the purpose of optimizing both intrinsic and extrinsic magnetic properties to improve the certain properties of the existing materials, and to discover new types of advanced soft magnets, it is unequivocally true that the particle morphologies in micro or nanostructural forms, and the alloy chemistry must be precisely controlled.

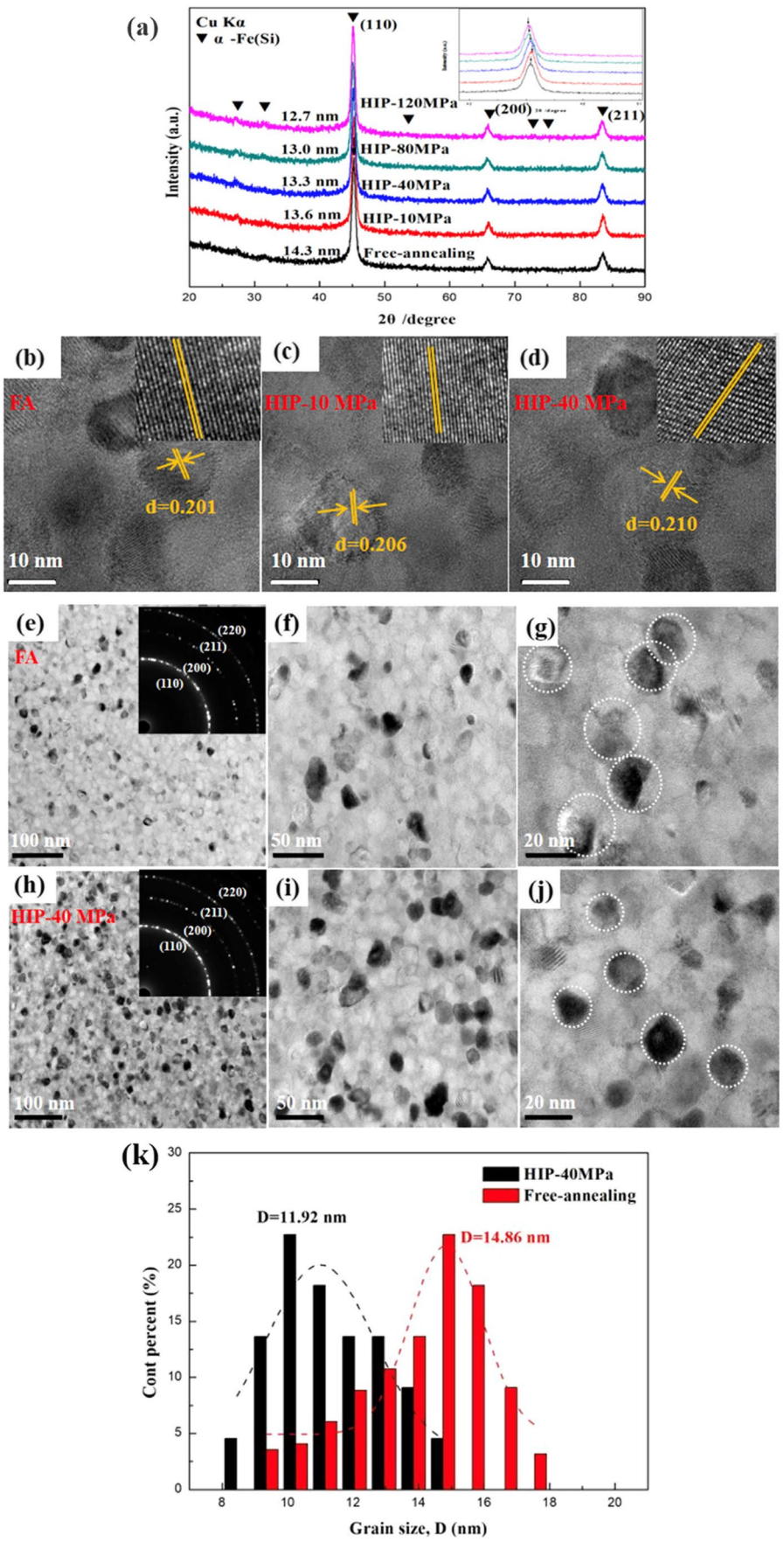

Fig. 2 Structural evaluation of $Fe_{73.5}Si_{15.5}B_7Nb_3Cu_1$ ribbons treated by free annealing (FA) and hot isostatic pressing (HIP). **a** XRD patterns. **b**–**d** High-resolution TEM images. **e**–**j** Bright field images inset with selected area diffraction patterns (SAED). **k**, **h** Grain size distributions. *Adapted with copyright permission from* [38]

2 Mechanical alloying technique

The mechanical alloying (MA) technique has a fascinating history of its own in becoming a solid-state processing technic. It began with the inventing work of J. S. Benjamin [42] for synthesizing metal alloys. Later on, MA evolved into a most economic and practicable means for the development of various soft magnetic amorphous nanocrystalline alloys. Primarily MA is a process of high energy ball milling of pure metal mixtures or metal composites. During the milling process, the alloying components undergo multiple change sequences like continuous welding, fracturing, and re-welding of powdered metal mixtures. With the MA method, it is possible to produce metal alloys of various kinds that are otherwise difficult or impossible to make using other conventional means. This method is very versatile and not limited to conditions like metal solubility or melting points of individual alloying components [43]. From the impacts of ball milling action, the particles of alloying metals undergo severe deformation forming flattened combined layer structures comprised of all constituents of the alloying metal particles creating lattice defects due to the deformation process, which in turn increases the diffusion rates and results in the formation of the alloy. Figure 3 shows the pictorial impression of the impacts from the milling media, the hardened steel balls, and the powder particles. The MA originally developed by J. Benjamin was to produce oxide dispersion strengthened Ni and Fe base superalloys needed for gas turbine applications. Further investigations since the pioneering work of Benjamin have also shown that the MA can be effectively applied for synthesizing metastable amorphous nanocrystalline or quasi-crystalline structures that used to be possible only by rapid solidification processes [44–48]. With the MA method, it is possible to produce alloyed products that are otherwise difficult or impossible to make using other conventional methods [14, 15, 49, 50]. As a matter of fact, compared to the rapid solidification processes, the ease of forming amorphous phases by MA, so to speak forming the glassy state of an alloy, is far superior. The glass formation range in the MA process is very broad, whereas in other conventional processes like the rapid cooling method, the glass formation region is restricted only to the eutectic region of the alloy of because kinetic limitations. Moreover, amorphization is very difficult using conventional means of alloy manufacture if the eutectic region of the melt is very wide and shallow. However, despite all advantages, there are concerns of entraining impurities during alloying process originating from the attritions from the vials and milling media. In order to prevent this, the use of vials and milling media made of hard metal alloys and ceramics composites can be helpful depending upon the end-use suitability. A yet another disadvantage is the loss in magnetization, which mainly stem from the defects occurred due to continuous impact and plastic deformations during MA. Anyway, annealing, as a post-process of MA, corrects the problem [7, 51].

The nanostructured materials like nanocomposites, nanocrystals, and amorphous-nanocrystalline structures synthesized by the MA method enable synthesizing materials with extraordinary properties by controlling the nanocrystalline sizes of the alloyed materials [7, 15, 52]. Moreover, using the MA method, it is possible to synthesize highly homogeneous materials of near full density with high purity and excellent mechanical and magnetic properties [19, 53]. In addition, using this method, a wide variety of materials can be synthesized in a wide variety of compositions [50, 54, 55]. In other words, by selecting appropriate alloying

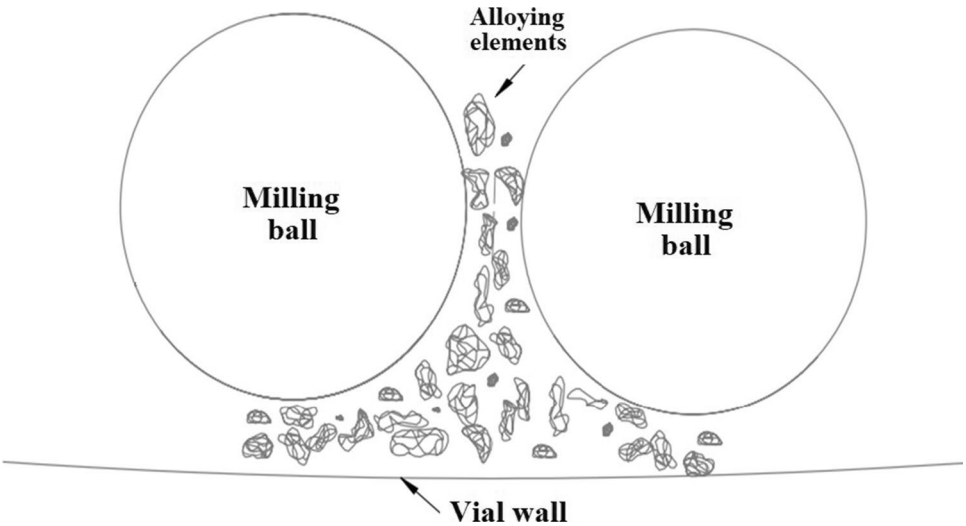

Fig. 3 A schematic representation of mechanical alloying process

parameters and choosing appropriate elements, a variety of nanomaterials like amorphous-nanocrystalline alloys, nanocrystalline alloys, nanocomposite alloys, and HEAs can be produced for soft magnetic applications, and for the application of hydrogen storage systems [4, 11, 14, 15, 56].

In MA, the obtained alloys can be controlled by adjusting the milling parameters [7]. Milled samples of the alloys can be collected at certain intervals during the milling process for the purpose of stepwise structural and material characterizations of the alloy in the making to provide a complete picture of the stepwise structural and morphological transformation as the alloying process continues, and also the changes occurred in their thermal and magnetic behaviors. The properties of the alloys thus formed by MA can be controlled by altering milling parameters and milling conditions if necessary [9, 14]. On the other hand, since the MA process only involves the solid-state processing of the metal powders, the amorphous phase formation criteria during the alloying stages are completely different from the other conventional methods like rapid solidification processes. The formation ability of the intermetallic components during the alloying process positively influences the scope of forming amorphous use of the alloy [7, 19, 57]. The more the intermetallic phase, the higher the ability of the alloy to be in the amorphous state. In the MA process, the amorphous phase occurs when the free energy (ΔG_a) of the amorphous phase formation is less than the formation free energy (ΔG_c) of the crystalline phase. Under the normal conditions, ΔG_c is generally higher than the ΔG_a meaning all alloying phases proceed via amorphization regardless of how transient it may be. However, in MA, when the process of alloy formation undergoes severe crystal deformations, dislocations, and lattice defects, the positive free energy of deformation (ΔG_d) further contributes to the ΔG_c making it even higher in value than the ΔG_a. In MA, the equation for the formation of free energy for the amorphous phase can therefore be expressed as $G_a < G_d + G_c$ [7, 14].

The free energy of the alloys increases enough to form an amorphous phase because of the reduction of grain size and dislocations, and also due to the presence of intermetallic phases during the MA process. However, it has been observed that when the milling time is increased, amorphous alloys showed a tendency to crystallize [14, 15, 58]. This situation has been named as mechanical crystallization. This phenomenon has provided a great opportunity for the emergence of a new class of materials, amorphous-nanocrystalline materials. In these materials, there exists a controlled proportion of both amorphous and crystalline phases displaying superior properties compared to either of these individual phases. For example, synthesis of either completely amorphous, amorphous-nanocrystalline, or fully crystalline materials can be possible by controlling both milling time and annealing conditions, particularly the annealing temperature and time. The amorphous phase formed during MA can undergo crystallization, which is also known as mechanical crystallization, which is unique to the MA, and this can happen when the milling of the amorphous phase is continued over a longer time. With the MA method, when parameters such as ball to powder ratio (BPR), milling medium, vial fill rate, mill speed, and milling period are selected appropriately, particle size reduction can continue steadily with the milling time. Moreover, it allows the production of nanostructured materials with high strength, excellent electrical, and magnetic properties. These are the most tangible benefits of MA and also the reasons why the MA method is preferred more over the other methods [7, 11, 15, 58]. By selecting the optimum parameters for the MA, amorphous-nanocrystalline alloys in a completely homogeneous structure can be successfully obtained. By using the MA method, three different alloys with $Co_{30}Fe_{30}Ni_{40}$, $Co_{30}Fe_{40}Ni_{30}$, and $Co_{40}Fe_{30}Ni_{30}$ compositions containing Co, Fe, and Ni were successfully synthesized by Betancourt et al. Based on the elemental maps of the synthesized alloy, it was observed that the content elements were homogeneously distributed in the alloy system after 7-h milling [59]. It is interesting to note in this context, depending on the methods of production used, alloys of identical compositions may differ greatly with respect to their mechanical, magnetic, and nanostructural characteristics. Even if the same production technique is used, those characteristics may also differ if one or more operating parameters are changed in a process. For example, in the MA, the parameters such as milling time, type of mills, rotating speed, milling temperature, milling medium, usage of process control agent (PCA), BPR, selected elements, annealing temperature, and time can significantly affect the properties of the resulting alloy [14, 60, 61]. By using the MA method, $Ni_{70}Co_{30}$ alloy was successfully produced by grinding for 0, 1, 5, 10, 15, and 25h by Abbasi et al. SEM images showed that the morphological structure and particle size of the alloy changed depending on the increasing MA time. It was also observed that the reduction in particle size and changes in particles shapes from an irregular to a spherical structure occurred by increasing MA time [62, 63]. In other words, as the milling time increases, face-centered cubic (FCC), body centered cubic (BCC), and amorphous phase transformations occur. However, it must be noted that milling more than the optimum milling period may cause impurities to develop and can damage the structural properties of the alloys formed. With the phase transformations occurring during MA, multiple significant changes may occur resulting different mechanical, microstructural, and magnetic properties [7, 63, 64].

The effect of milling time on magnetic properties was investigated by Alijani et al., for FeCoNiMnV HEA, which was alloyed for 96 h in a planetary mill with 350 rpm. It was observed that the M_s values of the as-made

alloy increased up to 48 h depending on the MA time, but this value decreased when the grinding process was continued. The highest M_s value of 100 emu/g was reached at the end of 48 h. However, as the milling continued, the M_s value started decreasing gradually. This situation has been attributed to the FCC-BCC phase transformations occurring in the alloy [65]. In another MA study, magnetic properties of Fe-Cr-Mn-N powders alloyed under a nitrogen environment were investigated. Interestingly it was observed that the increased milling time actually favored magnetic properties. As the MA milling time increased, the M_s increased and the H_c decreased. Milling under nitrogen atmosphere supported the glass-forming ability of the alloy. Ferromagnetic Co_2MnSi Heusler alloy was successfully synthesized when milled for 25 h of duration. It was shown that the Co_2MnSi phase was formed after 15 h of milling and the saturation magnetization reached a maximum after 20 h of milling duration. It was observed that as the milling time increased, the M_s value initially decreased from 112 to 75 emu/g and then again increased to the 95 emu/g and the H_c increased from 219 Oe to 269 Oe. The Co_2MnSi alloy was also successfully synthesized by Rabie et al. using the MA technique and it was seen that the M_s value reaches 120 emu/g by mechanically alloyed powders followed by post-annealing. It was reported that the measured H_c value decreased to 25 Oe. Based on these results, it is very apparent that the the prolonged MA time is not as effective as that of annealing for boosting the magnetic properties of the alloys [66]. $Co_xCrCuFeMnNi$ ($x = 0.5, 1.0, 1.5, 2.0$ mol) HEA was produced in a total of 50 h by performing 45-h dry and 5-h wet milling in ethanol in a planetary miller with a speed of 300 rpm. It was observed that the $Co_2CrCuFeMnNi$ alloy synthesized with $x = 2$ moles exhibited superior soft magnetic properties with M_s of 52 emu/g, and H_c of 14 Oe compared to other alloys formed with Co at molarities $x<2$. The reason for the improved magnetization characteristics was attributed to increasing amount of Co concentration in the alloy. In other words, as the amount of Co additive increased, the magnetic properties of the alloy improved. In addition to that, a single FCC phase was found to be formed by annealing the alloys at 900 °C, which further improved the magnetic properties. This established the importance of the annealing process for improving M_s values. It is worth noting in this respect, annealing at a lower temperature, e.g., 700 °C, the alloys can comprise two different phases which slowly transformed into single FCC phase as the temperature rises to 900 °C. It has been observed that the M_s values of the alloy consisting of single FCC phase are better than the alloys consisting of two phases [67].

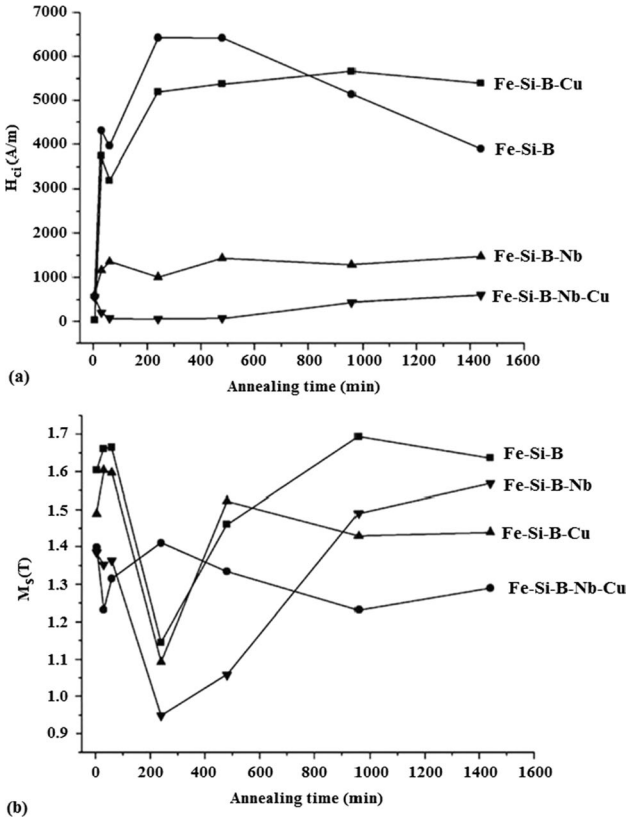

Fig. 4 **a** Effect of annealing on the structural and magnetic properties of the mechanically alloyed materials. **a** Effect of annealing time on H_c value for each composition. **b** Effect of annealing time on M_s value. *Adapted with copyright permission from* [70]

3 Subsequent annealing process

The annealing process, as a matter of fact, relieves the microstructure stresses and those complex structures can be reduced to a single phase with a simple structure, thus making significant improvements in mechanical and magnetic properties [14, 15, 61]. Using the MA method by Duan et al., FeCoNiCuAl alloy was successfully synthesized after 90 h of milling in a planetary-type mill with a speed of 300 rpm. The hysteresis curves of the synthesis alloy before and after annealing were examined in detail. It was observed that the synthesized alloy had a value of M_s approximately 73 emu/g before and 94.2 emu/g after annealing. These results definitely revealed that the annealing helps in improving the magnetic properties [68]. Nanocrystalline $Fe_{50}Co_{30}Ni_{20}$ was successfully synthesized by Raanei et al. with the desired properties by milling for 48 h followed by annealing at 450 and 650 °C. It was reported that the M_s (80.52 emu/g) of the samples milled for 48 h and annealed at 650 C was higher than the samples milled for 32 h and annealed at 650 °C (M_s 77.52 emu/g) [69]. In another study, Fe-Ni, Fe-Si, Fe-Co, Fe-Si-Ni, and Fe-Si-B alloys were synthesized using the MA

method. The annealing process was applied to each synthesized composition at 550 °C for various periods. Figure 4 shows the effect of the period of the annealing treatment on H_c and M_s values. It is seen that the highest M_s value was achieved after annealing for 1000 min in Fe-Si-B alloy, while the lowest H_c value belongs to the Fe-Si-B-Nb-Cu alloy [70].

4 Recently developed soft magnetic powder alloys

There are a large number of studies on many different types of magnetic materials and magnetic alloys produced by various production methods. In this section, a detailed search has been carried out on soft magnetic amorphous/nanocrystalline Fe, Co, Ni, FeCoNi-based alloys and HEAs synthesized by the MA method. Recently, amorphous/nanocrystal alloys and HEAs are the center of attention in the scientific world with their very good soft magnetic properties as well as other superior mechanical properties [71].

4.1 Fe-based alloys

Iron is the most widely used magnetic material with its reasonable cost, besides its high T_c (770 °C) and M_s (2.15 T). Synthesis of 50 different Fe-based soft magnetic amorphous alloys produced by various methods is there in the literature. The compositions of these alloys were mostly chosen as (Fe, Co, Ni) $_{70–85}$ (Si, B) $_{15–30}$ and they were synthesized in various particle sizes ranging from 20 to30 µm. Fe-based amorphous alloys have high M_s such as 1.5–1.63 T due to the lack of crystal structure [18, 72]. Their magnetic properties were improved by modifying the chemical compositions further for their applications in power distribution transformers, magnetic sensors, and amplifiers. Fe-based soft magnetic amorphous materials are of increasing importance in soft magnetic applications because of their low core losses, high magnetic permeability, and low H_c values. Amorphous materials can be easily magnetized and demagnetized because they do not have crystalline magnetic anisotropy and grain boundaries. This ensures that amorphous materials exhibit low energy and core loss and have excellent soft magnetic properties [36]. The amorphous alloys thus obtained can compete with other conventional soft magnetic materials in terms of soft magnetic properties [73]. Especially with the oil crisis in the 1970s, Fe-based amorphous alloys were synthesized at a level that could compete with grain-oriented Si-steels with their high M_s and low core losses, and were successfully used in power distribution transformers in the 1990s [11, 74]. Figure 5 briefly summarizes the Fe-based magnetic materials in a hierarchical order. As seen in the figure, Fe-based magnetic

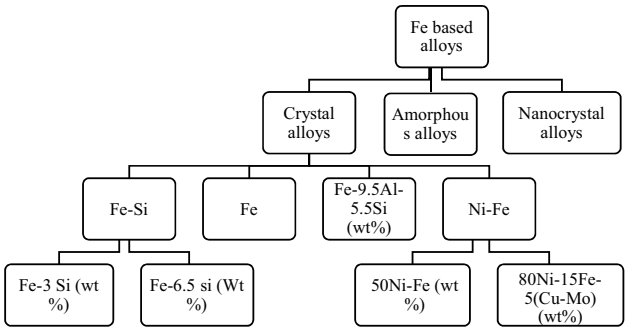

Fig. 5 Hierarchical representation of Fe-based magnetic alloys [74]

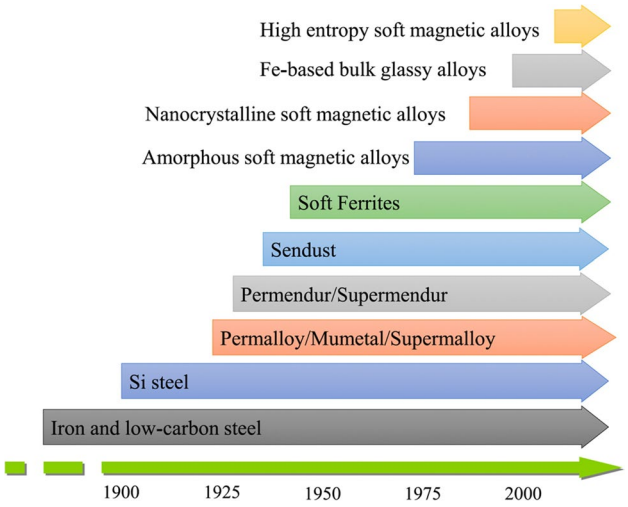

Fig. 6 Advancement and chronological evolution of soft magnetic alloys. *Adapted with copyright permission from* [9]

alloys are mainly examined in three groups. These groups are crystalline, amorphous, and nanocrystal alloys [74]. Crystalline alloys are the mostly used magnetic materials for over 100 HEAs. Amorphous alloys, on the other hand, are relatively new but have become a material of great interest due to their promising magnetic properties [7].

Figure 6 shows the advancement and chronological changes of some soft magnetic materials. As can be seen from the figure, Si steels together with iron and low carbon steels are still dominating as the soft magnetic materials. Amorphous/nanocrystal and other new material groups appear to be in the market later and their usage has been increasing but still far less than the conventional soft magnetic materials [9]. Amorphous alloys were first synthesized with rapid solidification (RS) methods and then successfully produced by MA with the development of the method [7, 18]. While alloys can be synthesized in limited quantities with the rapid solidification (RS) method, they can be synthesized in very large compositions and industrial

scales with the MA [7]. Nanocrystal alloys, another soft magnetic material group, were obtained by first annealing the amorphous materials at or above the crystallization temperature [75]. It has been shown by Yoshizawa et al. that these alloys have excellent magnetic properties. Fe-based amorphous alloys with soft magnetic properties could be synthesized in a controlled manner by applying an annealing process to amorphous alloys at a temperature above the crystallization. Moreover, nanocrystal alloys can be synthesized with desired properties using the MA method [72, 73, 76]. In another study, FeCo-based nanocrystalline alloys were synthesized by milling in a SPEX 8000 type mill for 10 h. In this study, $Fe_{50}Co_{50}$, $Fe_{70}Co_{30}$, $Fe_{69.97}Co_{30}B_{0.03}$, $Fe_{49.2}Co_{50}Zr_{0.8}$, $(Fe_{0.5}Co_{0.5})_{88}Cu_1Zr_7B_4$, $(Fe_{0.6}Co_{0.5})_{80}Cu_1Nb_5P_4B_{10}$, and $Fe_{62}Ni_{15}Cu_1Nb_2P_{14}B_6$ nanostructured/amorphous alloys were successfully synthesized with MA and heat treatment was applied to improve the magnetic properties of these alloys. The effect of annealing temperature on M_s and H_c is summarized in Fig. 7 [77].

It can be clearly seen that the highest M_s of 235 emu/g was achieved in $Fe_{70}Co_{30}$ after heat treatment at 800 °C. On the other hand, the H_c values of all the alloys are low ranging from 10 to 20 Oe after annealing regardless of their composition. Khazaei et al. were milled Fe-based $Fe_{0.7}Nb_{0.1}Zr_{0.1}Ti_{0.1}$ amorphous alloy for 60 h of duration. The wet milling process was applied using hexane as process cooling agent (PCA). It has been reported that the PCA add-on increases the amorphous phase formation while significantly changing the magnetic properties. It was observed that the PCA addition increased the M_s by approximately 43% and decreased the H_c by 50%. Similarly, improvement in magnetic properties has been also reported when milled powders are subjected to the annealing process [78]. İt has been well known that magnetic alloys are key materials for the future of the electronics industry. Recently developed transformers, inductors, coils, and filters require completely new types of alloys of superior properties. Among these new types of alloys, Fe-based Fe-Ni, Fe-Si, Fe-Co, Fe-Si-Ni, and Fe-Si-B alloys were successfully synthesized by Shokrollahi et al. using the MA method. It was seen that as the annealing time increased, the M_s value decreased first and then increased [70].

Fe-based alloys appear as the most important soft magnetic alloys due to their good magnetic properties. These alloys can be produced with two, three, or more components. The MA method stands out as one of the most suitable synthesis methods for soft magnetic Fe-based alloys because it enables the formation of supersaturated solid solutions, multi-phase structures, or amorphous alloys [70]. By using the MA method, alloys with very good magnetic properties such as nanocrystalline, amorphous, nanocomposite, and high entropy alloys can be synthesized to the desired quality. Table 1 summarizes the magnetic properties of Fe-based amorphous/nanocrystal alloys synthesized by the MA method showing that Fe-based alloys exhibit excellent soft magnetic properties.

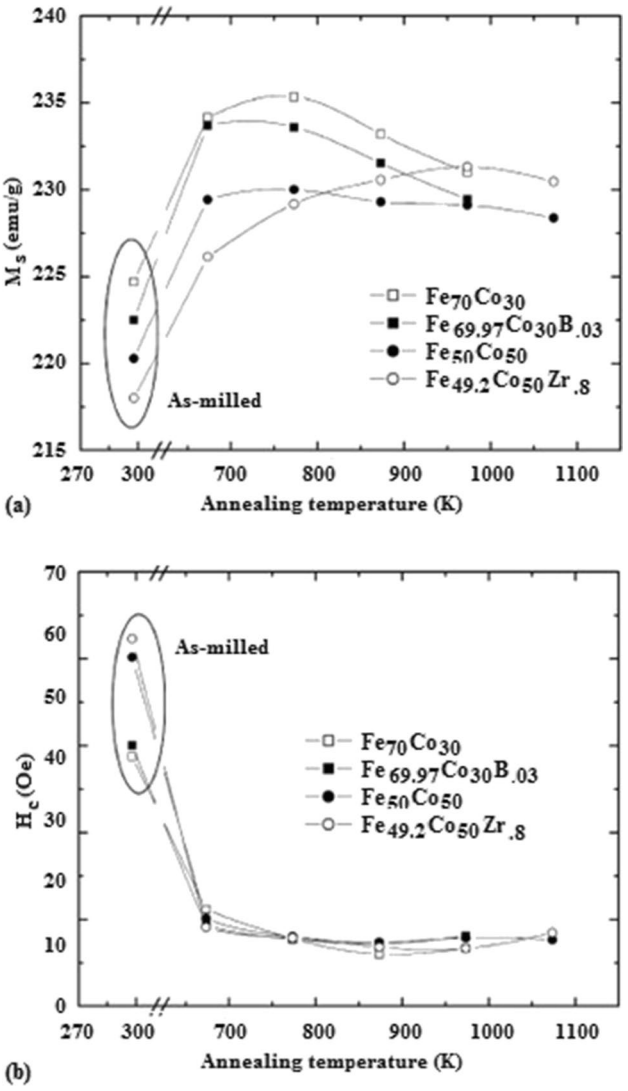

Fig. 7 The effect of annealing on the Fe-Co-based alloys produced by mechanical alloying. **a** M_s value. **b** H_c value. *Adapted with copyright permission from* [77]

4.2 Co-based alloys

Cobalt has been chosen as both main or additive element due to its high atomic magnetic moment. Moreover, the addition of Co in appropriate proportions significantly increases the M_s and T_c values of the alloys. Co-based $SmCo_5$ alloy was milled by adding Co in different proportions and the magnetic properties were investigated. It has been reported that a low H_c and high M_s were achieved by adding Co in different mass ratios and by annealing at 750 °C for 1 h. As the amount of Co increased in the

Table 1 Fe-based amorphous/nanocrystalline alloys recently produced by MA

Alloy composition		M_s (emu/g)	H_c (Oe)	Form	Ref.
$Fe_{80}P_{11}C_9$ milled for 120 h		158	16	Amorphous/nanocrystalline	[79]
$Fe_{92}Al_2Si_6$ milled for 30 h		186.5	16–20	Nanocrystalline	[80]
$Fe_{46}Co_{34}Ni_{20}$ milled for 9 h		169.0	1.2	Nanocrystalline	[81]
$Fe_{49}Co_{21}Mn_{10}Ti_{10}B_{10}$ milled for 100 h		138	33.0	Nanocrystalline	[82]
$Co_{60}Fe_{18}Ti_{18}Si_4$ milled for 50 h		89.68	155.08	Amorphous/nanocrystalline	[83]
$Fe_aNi_bNb_cZr_d$(a=31.3, b=48.7, c=0, d=20) milled for 20 h		70.6	17.0	Amorphous/nanocrystalline	[3]
$(Fe_{0.6}Co_{0.5})_{80}Cu_1Nb_5P_4B_{10}$ (milled for 10 h) (773 K/1 h)		165 185	68.3 16	Nanocrystalline	[77]
$(Fe_{0.5}Co_{0.5})_{88}Cu_1Zr_7B_4$					
Milled for 10 h 823 K/1h		162 190	81 38	Nanocrystalline	[77]
Fe_{80} $(NiZr)_7B_{12}Cu_1$					
SPEX milled for 80 h Planetary (P7) milled for 80 h		105.3 155.6	29.2 30.7	Nanocrystalline	[84]
Fe_{80} $Nb_7B_{12}Cu_1$					
SPEX milled for 80 h Planetary (P7) milled for 80 h		162.6 146.1	36.9 28.6	Nanocrystalline	[84]
$Fe_{75}Ta_5Co_{20}$					
20 h 70 h 120 h		145 130 132	4 2.75 3.4	Amorphous	[85]
$Fe_{46}Co_{34}Ni_{20}$ milled for 9 h annealed 300 K		175.6 169	4.5 3.3	Nanocrystalline	[81]
$Co_{40}Fe_{22}Ta_8B_{30}$ - Milled for 200 h		86	3.2	Amorphous	[86]
$Fe_{70}Cr_{10}Nb_{10}B_{10}$ alloy milled for 50 h and annealed at 972 K		~95	~76	Amorphous/nanocrystalline	[87]
$Fe_{70}Ti_{10}B_{20}$					
2.5 h 20 h 70 h		130 110 94	32 47 117	Amorphous/nanocrystalline	[88]
Fe-%45 Ni2-(milled for 4 h + %1 PCA) (milled for 48 h + %1 PCA)		138 3 163	14 ±3 –	Nanocrystalline	[89]
$Fe_{70}Cu_{30-x}Ni_x$					
X=	0	123	105	Nanocrystalline	[90]
	10	124	135		
	15	130	144		
	30	141	82		
Fe-%10 Ni milled for 36 h Fe-%20 Ni milled for 36 h		227 219	2.5 1.3	Nanocrystalline	[91]
$(Fe_{75}Al_{25})_{100-x}B_x$ (milled for 80 h)					
X =	0	-	-	Nanostructured	[92]
	5	-	-		
	9	130	35–40		
	12	128	30–40		
Fe-Si_x (milled for 20 h)					
X=	1.78 at.%	197	18	Nanocrystalline	[93]
	5.08 at.%	186	22.5		
	8.04 at.%	182.5	17.5		
$Fe_{49}Co_{49}V_2$		186	56		

Table 1 (continued)

Alloy composition		M_s (emu/g)	H_c (Oe)	Form	Ref.
Milled for	2 h	177	48	Nanostructured	[94]
	10 h	193	56		
	16 h	174	52		
	32 h	185	61		
	56 h	182	65		
	126 h	182	53		
$(Fe_{67}\ Ni_{33})7_0\ Ti_{10}\ B_{20}$					
milled for 120 h		105.3	36.7	Nanostructured	[62]
Milled for 120 h and annealed at 1044 C		90.2	77.3		
$Fe_{42}Ni_{28}Zr_8Ta_2B_{10}C_{10}$					
milled for 198 h		93.9	33.3	Amorphous/nanocrystal	[95]
milled for 176 h		82	24.0		
milled for 176h and heat 500 C		77.1	11.7		
milled for 176h and heat 650 C		87.6	25.4		
$Fe_{70}Ta_5Si_{10}C_{15}$					
milled for	120 h	93	34.1	Amorphous/nanocrystal	[96]
	120 h (673 K)	100	17.3		
Annealed	120 h (743 K)	105	27.0		
	120 h (848 K)	116	28.5		
	120 h (993 K)	119	28.7		
$(Fe_{0.7}Co_{0.3})_{100-x}Si_x$ [milled for 72 h]					
X=	0	223	42	Nanocrystalline	[97]
	5	213	41		
	10	199	42		
	15	185	49		
	20	162	52		
$Fe_{95}B_5$ (milled for 50 h)					
Before washing		21	191		
After washing		28	179		
$Fe_{85}B_{15}$ [milled for 50 h]				Nanocrystalline	[98]
Before washing		9.5	237		
After washing		14	200		
$(Fe_{50}Ti_{25}Al_{25})_{70}B_{15}P_7C_6Si_2$ [milled for 30 h]		30	125	Amorphous/nanocrystalline	[99]
$(Fe_{50}Ti_{25}Al_{25})_{70}B_{15}P_7C_6Si_2$-$Co_{20}$ [milled for 20 h]		82	129		
$(Fe_{85}Ni_{15})_{100-x}Cu_x$ (milled 72 h)					
X=	0	150	35	Nanocrystalline	[100]
	0.5	156	29		
	1.5	159	62		
	3	166	40		
	5	160	41		
Fe–16.5Ni–16.5Co					
milled for 50h		15.1	700	Nanopowder	[101]
Reduce under hydrogen		42.9	116.2		
$Fe_{84}Nb_7B$					
milled for 35 h		155	360	Nanocrystalline	[102]
Milled for 35 h and annealed at 350 C/30 min		-	120		
$FeSi_{10}Cr_{10}$					
Milled for 30 h		151	31.4	Nanocrystalline	[103]
$[Fe_{50}(Co_{50})]$–6.5 wt% Si					
Milled for 18 h		188	87	Nanocrystalline	[104]

Table 1 (continued)

Alloy composition		M_s (emu/g)	H_c (Oe)	Form	Ref.
$Fe_{65}Co_{35}$ milled for 80 h		185	25.3	Nanocrystalline	[105]
$(Fe_{65}Co_{35})_{80}$ Si_{20} (Milled for 80 h)		110	43.8		
$(Fe_{65}Co_{35})_{90}$ Si_{10} milled for 80 h		150	35.1		
$Fe_{75}Si_{25}$					
milled for 80 h		150	30	Nanocrystalline	[106]
Fe-%10Ni					
Milled for 36		213	5.28	Nanocrystalline	[107]
Fe-%20Ni					
As milled for 36 h		200	5.03		
Fe-%10 Ni milled for 36 h		209	32.5	Nanocrystalline	[108]
Fe-%10Si milled for 36 h		199	30.0		
Fe-%10Al milled for 36 h		205	21.9		
$Fe_{75}Ta_5Co_{20}$					
20 h		145	4	Amorphous	[85]
70 h		130	2.7		
120 h		132	3.4		
$Fe_{72-x}Co_xCr_{28}$ ($10 < X < 22$)					
Milled for 20 h		175	115		
(x=10) annealed	560	170	87	Nanocrystalline	[109]
	600	165	88		
	620	150	87		
	640	135	87		
(x=14) annealed	560	175	135		
	600	168	113		
	620	138	100		
	640	135	89		
(x=22) annealed	560	165	150		
	600	150	125		
	620	120	101		
	640	100	100		
$Fe_{50}Co_{25}Ni_{15}X_{10}$ (milled 100h)					
FeCoNi milled for 100 h		125	13	Amorphous/nanocrystalline	[110]
X = B amorphous		160	48		
X= B crystalline		95	58		
X= Si		160	93		
$(Fe_{85}Ni_{15})_{97}Al_3$					
As milled	0 h	155	-	Nanocrystalline	[111]
	4 h	180	-		
	16 h	185	-		
	32 h	195	-		
	64 h	185	-		
$(Fe_{70}Al_{30})_{100-x}Si_x$ [milled for 72 h]					
X (at.%)=	0	150	37	Nanocrystalline	[112]
	5	125	22		
	10	85	21		
	15	75	23.5		
	20	45	42.5		
Fe-49 wt% Co-2 wt% V					
Milled for 45 h	300 K	211	66.6	Nanocrystalline	[113]
	600 K	210	43.9		
	900 K	225	6.7		
Co_3C-$Co_{0.35}Fe_{0.65}$ milled for 72 h		189	70	Nanostructured	[114]
$Fe_{70}Zr_{30}$					

Table 1 (continued)

Alloy composition		M_s (emu/g)	H_c (Oe)	Form	Ref.
Milled for	8.5 h (magnetic properties calculated at 100 K)	75	87.9		
	16 h (magnetic properties calculated at 100 K)	80	43.9		
	50 h (magnetic properties calculated at 100 K)	72	12.6	Amorphous	[115]
Milled for	8.5 h (magnetic properties calculated at 300 K)	40	213.6		
	16 h (magnetic properties calculated at 300K)	30	188.5		
	50 h (magnetic properties calculated at 100 K)	20	173.4		
$Fe_{80}Nb_{10}B_{10}$ (Milled for 60 h)					
Annealed at	400 K	77	-	Amorphous	[116]
	800 K	92	-		
	1200 K	160	-		
$Fe_{46}Co_{34}Ni_{20}$ [milled for 15 h]					
At 300 K (post-thermal treatment)		190	25.1	Nanocrystalline	[117]
Annealed at	300 K	160	-		
	840 K	171	-		
$Fe_{75}Ta_5Si_{10}C_{10}$					
Milled for	70 h	152	30.7		
	90 h	146	45.7		
	120 h	148	46.6		
$Fe_{70}Ta_5Si_{10}C_{15}$					
Milled for	70 h	145	29.6	Nanocrystalline	[118]
	90 h	96	30.6		
	120 h	93	34.1		
$Fe_{65}Ta_5Si_{10}C_{20}$					
Milled for	70 h	120	28.8		
	90 h	90	27.4		
	120 h	86	26.9		
Fe-15 wt% Si					
Milled for (4 h, 8 h) and annealed at 400 K	4 h	130	-		
	8 h	134	-	Nanocrystalline	[119]
Milled for (12 h) and annealed at 400 K	12	132.5	-		
Milled for (16 h, 20 h) and annealed at 400 K	16 h	131	-		
	20 h	134	-		

alloy, the M_s value also increased accordingly [120, 121]. Whether Co-based alloys are produced by fast cooling methods or by the MA method, it has been observed that the Co addition improves the magnetic properties [9, 122]. It has been observed that the 49Fe-49Co-2V alloy obtained by RS method exhibits excellent magnetic properties with high μ (4000–8000) and M_s (2.4 T) [13]. After the amorphous alloys were obtained by rapid cooling, these alloys attracted the attention of scientists because of their extraordinary properties. In amorphous alloys, it is not possible to repeat a certain structure or geometric shape as in crystal alloys. In other words, their atoms are random arranged. Figure 8 shows the XRD measurement as-milled Ti-Ni-Co-B powders after milling from 4 to 190 h. It is very interesting that after 190 h of milling, there is no observed Bragg reflections showing that the structure

completely becomes amorphous. Moreover, since the crystallite defects in amorphous alloys are not encountered as much as in crystalline alloys, these structures exhibit unusually superior mechanical and magnetic properties [7, 69, 75]. Thanks to these good soft magnetic properties, amorphous/nanocrystal alloys have been considered as an alternative to conventional soft magnetic alloys. For this purpose, in addition to the RS method, the MA method, in which amorphous/nanocrystal alloys in various compositions can be synthesized easily, has also been used to synthesize amorphous/nanocrystal alloys [56, 57, 74, 122].

In another study, dependence of M_s and H_c values on the milling time for the amorphous $Co_{60}Fe_5Ni_5Ti_{25}B_5$ alloy was investigated by Avar et al. It was observed that both M_s and H_c decreased substantially as the milling time increased. In addition, it was also observed that the annealing process did not improve the magnetic properties of that amorphous alloy. This anomaly was mainly due to the crystallinity occurred during the amorphous phase formation [17]. With the MA method, Fe- and Co-based amorphous-nanocrystalline alloys have been successfully synthesized on a large scale. Co-based $Co_{49}Ni_{21}Ti_{10}B_{20}$ amorphous alloy was synthesized by the MA method by milling for 190 h. Annealing process has been applied to the resulting alloy and its effect on magnetic properties has been observed. The results showed that the M_s of the 190 h as-milled alloy was lower than the M_s of the annealed alloy. On the other hand, the H_c increased significantly with the annealing. M_s and H_c values of Co-based amorphous $Co_{49}Ni_{21}Ti_{10}B_{20}$ alloy produced by MA were investigated in detail by Raanei et al. It was reported that while the M_s started decreasing after the first 40 h, there was a continuous decrease in the H_c with the increasing milling time [69]. Although Co-based alloys have very good soft magnetic properties, Fe-based

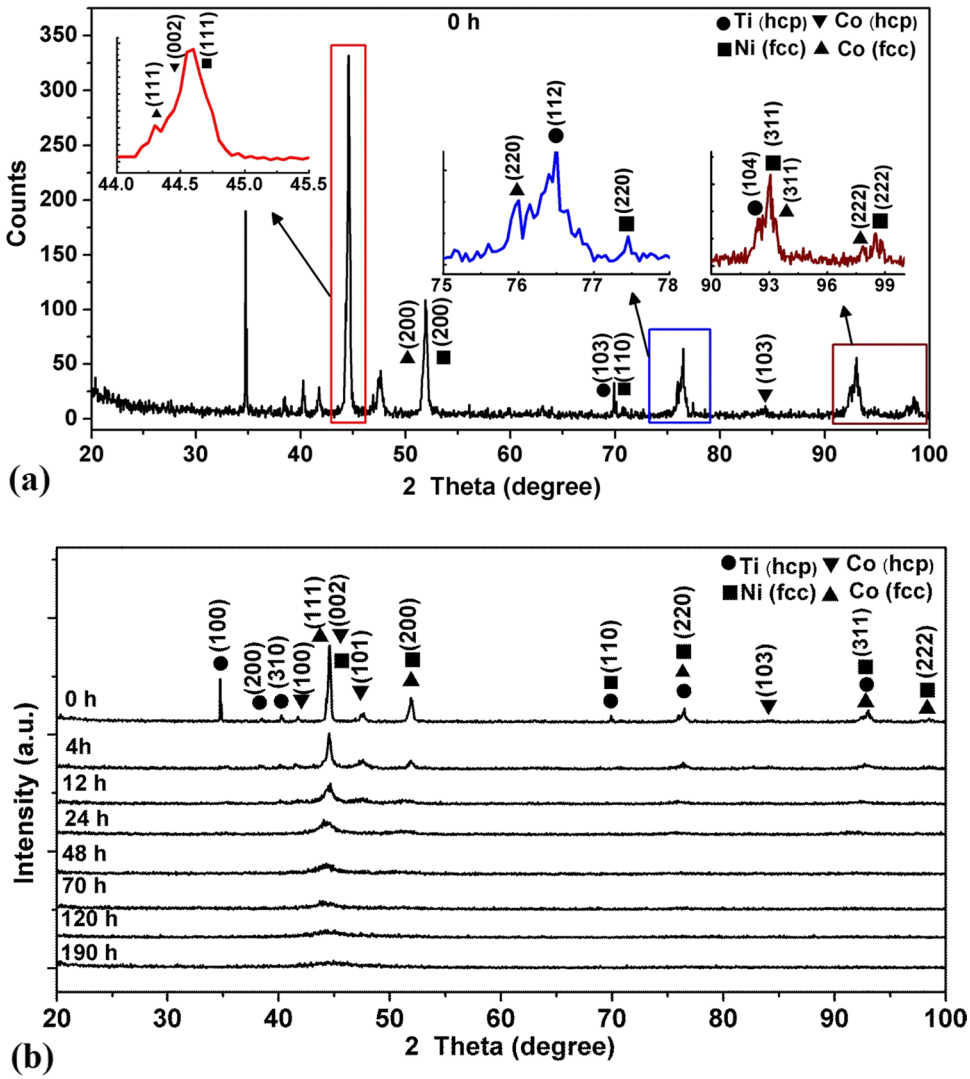

Fig. 8 XRD plots of the **a** mixture powders before milling process. **b** $Co_{49}Ni_{21}Ti_{10}B_{20}$ amorphous alloy obtained as a result of 190 h-milling process. *Adapted with copyright permission from* [69]

Table 2 Co-based amorphous/nanocrystal alloys produced with MA and their magnetic properties

Alloy composition		M_s (emu/g)	H_c (Oe)	Form	Ref.
$Co_{40}Fe_{22}Ta_8B_{30}$					
Milled for 200 h		77	40.2		
Annealed at	613 K	70	15.1	Amorphous	[86]
	723 K	68	16.3		
	773K	56	15.1		
60Co–26Fe-14Al					
Milled for	7 h	149	24.7		
	15 h	146	25.4	Nanocrystal	[124]
	30 h	144	24.4		
	50 h	141	24		
$(Co\text{-}Ni)_{70}Ti_{10}B_{20}$				Amorphous/nanocrystal	[125]
Milled for 190 h		78.4 ±3.9	39.3 ±1.9		
Annealed at 493 C		71.6 ±3.5	120.6		
Co_2MnAl (milled for 5 h)		105	25	Amorphous/nanocrystal	[126]
Co2B (milled for 20 h)					
(rpm)	250	48.9	337.41	Nanocrystal	[127]
	300	38.4	248.26		
	350	42.7	223.58		
$Co_{70}Fe_4Ni_2Si_15B_9$					
MA (40h)		43	-	Nanocrystal/amorphous	[128]
573 K /2h annealed		103	-		
573 K/3h annealed		100	-		
$Fe_{49.2}Co_{50}Zr_{0.8}$ milled for 10 h					
873 K/1h annealed		232	11.5		
$Fe_{50}Co_{50}$				Nanocrystal	[77]
Milled for 10h		221	58		
873 K/1h annealed		230	12.4		
$(Fe_{0.6}Co_{0.5})_{80}Cu_1Nb_5P_4B_{10}$					
milled for 10 h		165	68.3	Nanocrystal	[77]
annealed at 773 K/1 h		185	16		
$Co_{70}Si_{15}B_{15}$ (milled for 2h)		135	147		[129]
(36 h milled)		100	118	Nanocrystal	
(72 h milled)		95	114		
$Fe_{45}Co_{45}Ni_{10}$					
Milled for	10 h	169	35		
	20 h	185	36	Nanostructured	[130]
	35 h	180	39		
$Co_{70}Fe_4Ni_2Si_{10}B_9Ti_5$					
Milled for 40 h		59	-		
$Co_{70}Fe_4Ni_2Si_{10}B_9Zr_5$					
Milled for 40 h		60	-		
$Co_{70}Fe_4Ni_2Si_{15}B_9Zr_5$				Amorphous/nanostructured	[131]
Milled for 40 h		58	-		
$Co_{70}Fe_4Ni_2Si_{15}B_9Ti_5$					
Milled for 40 h		55	-		
$Co_{57}Fe_{13}Nb_8Ta_4B_{18}$					
Milled for 160 h		115.5 ± 5.5	123.4± 6.1		
Milled for 160 h and annealed at 243 C		119.7 ± 6	11.6 ± 5.5	Nanocrystalline	[132]
Milled for 160 h and annealed at 427 C		139.1 ± 7.5	136.8 ± 6.5		

Table 2 (continued)

Alloy composition		M_s (emu/g)	H_c (Oe)	Form	Ref.
$(Co_{75}Ti_{25})_{100-x}Fe_x$ milled for 60 h					
X=	0	0.61	-		
	2	0.70	-		
	5	0.71	-		
	7	0.72 (T)	-		
	10	0.87	-	Amorphous	[133]
	15	0.94	-		
	20	1.01	-		
$Co_{71}Ti_{24}B_{5,}$					
Milled for 36 h		1.01 (T)	35.9		
As consolidated (subsequent hot pressing)		0.96	36.7	Amorphous	[134]
$(Fe\text{-}Co)_{70}\ Mn_{10}\ Ti_{10}\ B_{10}$					
As-milled 35 h		113	50		
As-milled 35 h and annealed at 600 C		124	40		
As-milled 35 h and a nnealed at 900 C		119	43	Nanocrystalline	[135]
As milled 100 h		107	189		
As milled 100 h and-annealed at 600		125	132		
As milled 100 h and-annealed at 900		139	33		
$Co_{80-x}Ta_xSi_5C_{15}$ (x=0, 5)					
X= 0 (Milled for)	20 h	107	56.5		
	45 h	103	47.7	Amorphous/nanocrystalline	[136]
	120 h	100	56.5		
X= 5 (Milled for)	20 h	67	57.8		
	45 h	40	18.8		
	120 h	40	18.6		
$(Co_{75}Ti_{25})_{100-x}B_x$ (milled for 50 h					
X=	10	0.74	212.3	Amorphous	[137]
	20	0.95	182.2		
	30	0.85	221.2		

alloys are preferred because the Co is an expensive material. However, the low amount of Co addition is highly preferred in many alloy systems as it improves magnetic and electrical properties significantly [9, 123]. Table 2 summarizes the contribution of the Co addition to magnetic properties of recently synthesized Co based alloys by the MA method.

4.3 Ni-based alloys

It has been investigated that when Ni is added to an alloy system, it usually makes a significant improvement in the magnetic properties of the alloy. Ni-based alloys are widely used in inductance cores and transformers, especially in power generation transformers, thanks to their high M_s, permeability, and electrical resistance [9, 52]. In soft magnetic alloy, Ni content is generally preferred at 30% or above in order to increase the T_c. According to Ni content, in Ni-based alloys, the highest permeability was obtained in alloys containing 80% Ni, the highest M_s at 50% Ni and the highest electrical resistance at 30% Ni. Properties such as M_s, permeability, and electrical resistance are known to be the most important properties for soft magnetic materials [13, 124]. Since these three can be obtained at a very high value, Ni-based alloys have a wide range of uses for soft magnetic applications [138]. Furthermore, Ni-based Ni-Zn and Ni ferrites are widely used in electronic devices and the telecommunications industry today [52]. Moreover, Ni-Zn ferrites are known to be highly preferred useful materials in transformer cores for high-frequency applications and in various electronic devices [52, 139–141]. Because Ni-based alloys have various usage areas, the production techniques are still improving. With the development of technology, the increase in energy needs has become the main goal to minimize energy losses in areas such as power generation and distribution transformers where energy losses are intense [142, 143]. To reduce these losses, advanced materials with better soft magnetic properties are needed than currently used counterparts such as Si steels and low carbon steels [9, 124]. From this point of view, it appears that amorphous/nanocrystalline alloys have much better

Table 3 Ni-based amorphous/nanocrystal alloys recently synthesized by MA

Alloy composition		M_s (emu/g)	H_c (Oe)	Form	Ref.
$Ni_{58}Fe_{12}Zr_{10}Hf_{10}B_{10}$					
Milled for 190 h		30	20		
Milled for 190 h and annealed at 450 for 2h		40	5	Amorphous	[146]
75wt% Ni-Fe					
16 h		81	-		
32 h		56	-	Nanocrystalline	[147]
64 h		12	-		
100 h		7	-		
CoNi milled for 10 h					
Before annealing		111.4	127.7		[148]
				Nanocrystalline	
After annealing (750 C/2h)		129.5	30.9		
Ni-Zn ferrit-as milled for 40 h					
Sintered at 1200 °C (10 °C/dak) 3 h		54	25	Nanocrystalline	[149]
$Ni_{70}Co_{30}$					
Milled for	5h	96	34		
	10h	106	31	Nanocrystalline	[150]
	15h	107	31		
	25h	87	30		
$Cu_{50}Ni_{50}$					
5h		3	50	Nanocrystalline	[151]
15h		6	25		
30h		49	10		
$NiFe_2O_4$ milled for 50 h					
Annealed at	1018 K	40.6	0.164 (T)	Nanocrystalline	[54]
	1108 K	46.2	0.092 (T)		
	1198 K	52.8	0.011 (T)		
$Fe_{42}Ni_{40}B_{18}$ Milled for 100 h		0.1 (T)	15.0	Nanostructured	[152]
After heat treatment		0.7	20.1		
$Fe_{40}Ni_{38}B_{18}Mo_4$ milled for 100 h		1.2 (T)	17.46	Nanostructured	[152]
After heat treatment		1.2 (T)	8.17		
$NiFe_2O_4$					
Milled for	8 h	24.35	0.351 (T)	Nanocrystalline Ni ferrite	[153]
	annealed 973K	34.55	0.107 (T)		
Annealed at	1073K	49.22	0.024 (T)		
	1273K	53.62	0.013 (T)		
$NiZnFe_2O_4$					
Milled for 60 h		52.97	129.95		
Annealed 800 C/4 h		83.22	43.8	Nanocrystalline	[154]
$Ni_{0.3}Zn_{0.7}Fe_2O_4$					
Milled for 60 h		39	-	Nanocrystalline	[155]
Annealed 800 C/4 h		46	-		
$Ni_{1-x}Mn_xFe_2O_4$ (milled for 2 h)					
X=	0	12	-		[156]
	0.3	40	-	Nanocrystalline/nanosized	
	0.5	36	-		
	0.7	24	-		
$_{50}i_{50}$					
$Fe_{50}Ni_{50}$ milled for 50 h		120	-	Nanocrystalline	[157]
$NiFe_2O_4$					

Table 3 (continued)

Alloy composition		M_s (emu/g)	H_c (Oe)	Form	Ref.
milled for 1 h and 30 h		53	-	Nanocrystalline	[158]
		32	-		
$Fe_{50}Ni_{50}$					
Milled for	5 h	148	37		
	25 h	145	16	Nanocrystalline	[159]
	50 h	133	18		
$Ni_{0.5}Co_{0.5}Fe_2O_4$ (milled for 2h)		56	920	Nanocrystalline	[160]

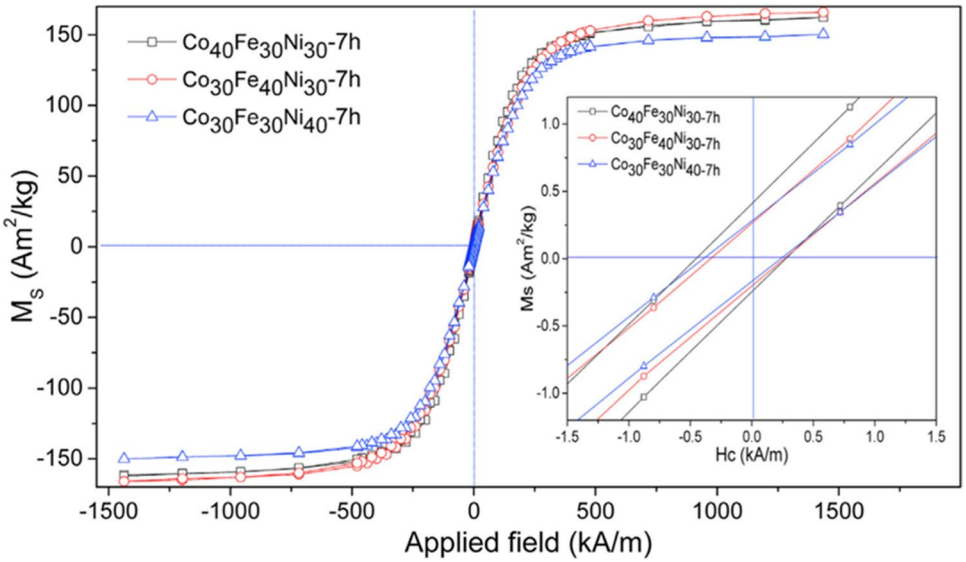

Fig. 9 Hysteresis curves of Fe-Co-Ni ternary alloys milled for 7 h. *Adapted with copyright permission from* [59]

magnetic properties than other conventional soft magnetic materials [7, 21, 144]. These alloys are produced using both RS and the MA method. By using the MA method, Ni, Fe, and Co-based amorphous/nanocrystal alloys could by easily synthesized with a wide variety of compositions and desired properties [7, 9]. The nanocrystal ($NiFe_2O_4$) alloy was successfully synthesized by the MA method using a planetary type mill and then annealed to improve the magnetic properties by V. Sepelak at al. When the hysteresis curve was examined, it was seen that the M_s of the as-milled sample was 33.2 emu/g, and the H_c was 0.245 T. On the other hand, these values were measured of the milled sample followed by annealing at 1198 K as 52.8 emu/g and 0.011 T, respectively. Results show that this Ni-based alloy exhibits excellent soft magnetic properties after milling and annealing [145]. In another study, the nanocrystal Fe-10% Ni and Fe-20% Ni alloys were successfully synthesized by the MA by Hamzaoui et al. It has been reported that the M_s of the former alloy (227 emu/g) was higher than the latter second (219 emu/g). On the other hand, H_c was 200 and 110 A/m, respectively. Thus, the addition of Ni decreases the H_c while Fe increases the M_s [83]. Table 3 depicts the Ni-based amorphous/nanocrystal alloys recently produced with MA summarizing that Ni-based alloys exhibit excellent soft magnetic properties. This enables Ni-based alloys to be used in electronic devices, power generation transformers, telecommunications industry, inductance cores, and many other electronic devices [21, 54, 140].

4.4 FeCoNi-based alloys

It is known that alloys based on Fe, Co, and Ni elements have excellent magnetic properties. Fe-Co alloys containing atomically about 30% Co show good soft magnetic properties while adding 10–20% Ni by weight improves the electrical resistance and permeability significantly [69]. Fe-Co-Ni ternary alloys are frequently used in file storage devices, energy storage, power converter, signal transmission, and quantum devices thanks to their magnetic properties such as good electrical resistance, high permeability, and M_s, low H_c [60, 101, 161]. When Co and Ni elements are added to Fe-based alloys, it improves the high-temperature magnetic properties of the alloys. Fe-Co-based alloys come to the fore with their high T_c and M_s. On the other hand, Fe-Ni-based

Table 4 FeCoNi-based amorphous/nanocrystal alloys synthesized by MA

Alloy composition		M_s (emu/g)	H_c (Oe)	Form	Ref.
$Co_{40}Fe_{30}Ni_{30}$ milled for 7h		162	0.365		
$Co_{30}Fe_{40}Ni_{30}$ milled for 7h		166	0.296	Nanocrystalline	[59]
$Co_{30}Fe_{30}Ni_{40}$ milled for 7 h		150	0.306		
$Co_{60}Fe_5Ni_5Ti_{25}B_5$					
Milled for 0.5 h		108	129		
Milled for 1.5h		104	159	Amorphous	[17]
Milled for 3.5 h		57	-		
Milled for 7h		53.4	7.6		
FeCoNi milled for 100 h		120	13		
FeNiCoB (nanocrystalline) milled for 100 h		77	59	Amorphous/nanocrystalline	[110]
FeCoNiB-(amorphous) milled for 100 h		160	50		
FeCoNi $(Mg\text{-}Si)_x$ milled for 25 h					
X=	0.0	94.1	91.6	Nanocrystalline	[163]
	0.1	142.4	30.2		
	0.2	30.0	295.7		
FeCoNi $(Mg\text{-}Si)_x$ milled for 25 h					
X=	0.0	125.5	46.8		
	0.1		16.5	Nanocrystalline	[41]
	0.2	234.0	23.2		
		266.6			
$Fe_{40}Co_{30}Ni_{30}$ milled for 15 h					
In Ar		146	4.3		
In air at 300 K		138	5.5		
Annealed In Ar at 660K		147	3.3	Nanocrystalline	[162]
Annealed In air at 660K		144	4.1		
Annealed In Ar at 840K		167	3.4		
Annealed In air at 840K		167	4.3		
FeCoNiSi milled for 100 h		163	90	Amorphous/nanocrystalline	[110]
$(FeCoNi)_{70}Ti_{10}B_{20}$					
Milled for 50 h		107.2	33	Amorphous	[164]
milled for 50 h and annealed 350C		119.2	13		
milled for 50 h and annealed 700 C		52.6	72		
FeNiCo					
	5 h	116.2	60.6		
	10 h		36.7		
milled for	15 h	121.8	65.4	Nanocrystalline	[165]
	20 h	122.0	59.4		
	25 h	125.4	46.8		
		125.5			

alloys come to the fore with their electrical resistances and high μ values. Fe-Co-Ni ternary amorphous/nanocrystal alloys are very popular for soft magnetic applications, as they have excellent magnetic properties containing the combination of properties of each element [60, 82]. Fe-Co-Ni amorphous/nanocrystal alloys with good magnetic properties, which are important for soft magnetic applications, can be produced comfortably in various compositions with desired properties using the MA method [162].

Figure 9 shows the hysteresis curves of Fe-Co-Ni ternary nanocrystal alloys synthesized using the MA method. It is seen that the nanocrystal $Fe_{30}Co_{40}Ni_{30}$ alloy subjected to the milling for 7 h has the highest M_s (162 emu/g) and the lowest H_c value [59]. MA parameters such as milling temperature, milling time, milling vial type and volume, the ball to powder ratio, milling environment, and PCA significantly affect the structural, mechanical, and magnetic properties of the alloy [162]. When these parameters are selected appropriately, the synthesis of the desired material can be easily controlled. MA method offers the opportunity to synthesize alloys in a wide variety of compositions compared to other methods [7]. Table 4 shows the composition and magnetic

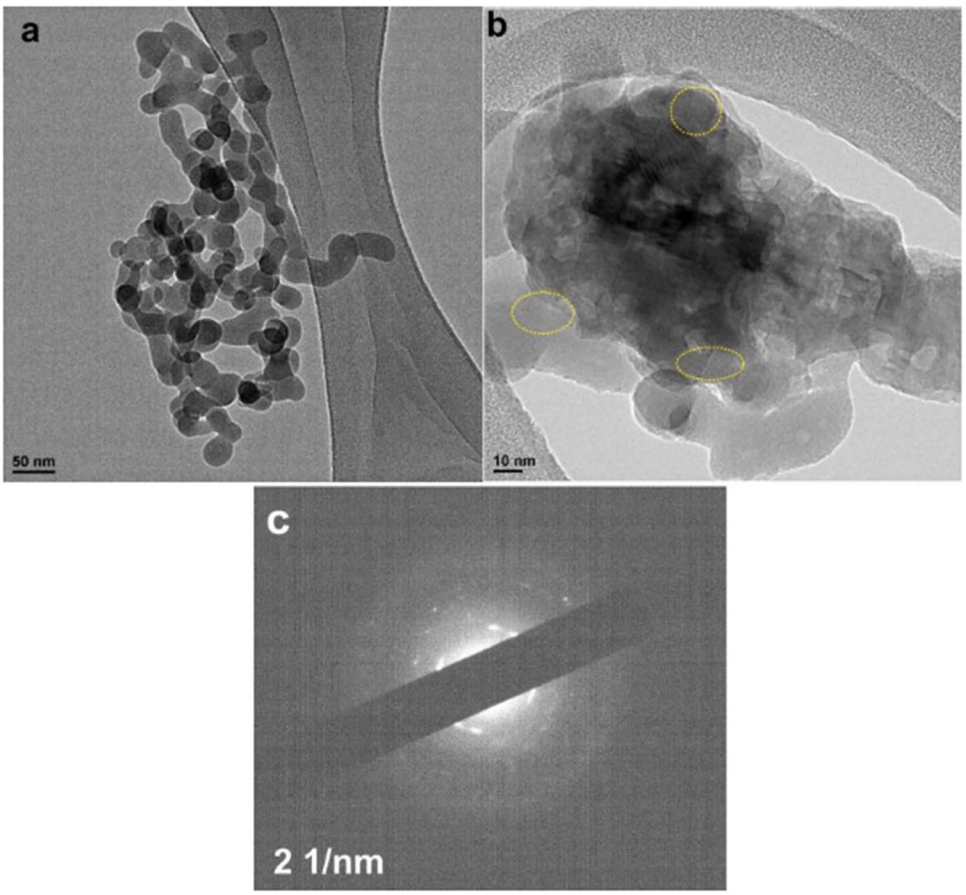

Fig. 10 **a**, **b** TEM images with **c** SAED pattern of the $Co_{64}Fe_{21}Zr_{10}Cu_5$ (at.%) alloy after 60 h-milling. *Adapted with copyright permission from* [166]

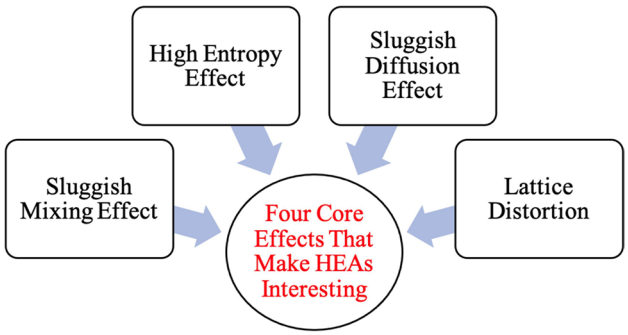

Fig. 11 Four core effects that make HEAs interesting

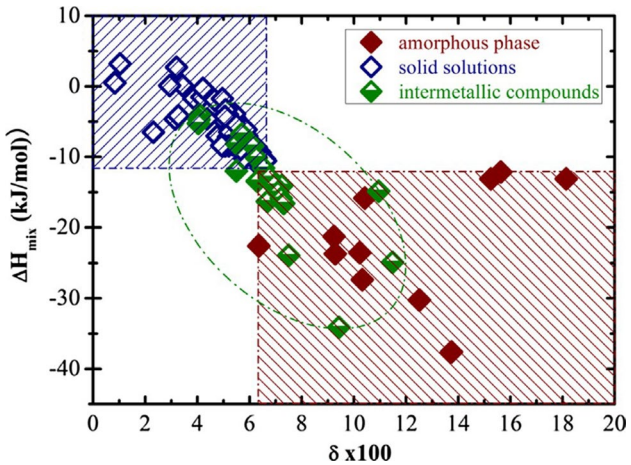

Fig. 12 Representation of phases corresponding to $\Delta H_{mix} - \delta$ values. *Adapted with copyright permission from* [170]

properties of Fe-Co-Ni-based amorphous/nanocrystal alloys synthesized by the MA method, summarizing promising magnetic properties of the Fe-Co-Ni alloy.

In addition, as it is known in amorphous and nanocrystalline materials reducing crystallite sizes in the alloy is important for its soft magnetic properties. Considering this fact, many studies continue to be carried out on the amorphous and nanocrystalline magnetic alloys using mechanical alloying. In one of these studies, Hajipour et al. reported the dependence of the magnetic properties on the crystallite size of the alloys. They obtained the $Co_{64}Fe_{21}Zr_{10}Cu_5$ (at.%) alloy powder in nanocrystalline form after 60 h of milling. As can be seen from the TEM results in Fig. 10, the nano-sized particles, the nanocrystallites, of irregular morphology were embedded in the amorphous structure of the alloy. The

areas of embedded amorphous structures are marked by circles. The selected area electron diffraction (SAED) image of the alloy shows the combination of both amorphous and nanocrystalline forms [166].

4.5 High entropy alloys

High entropy alloys (HEA) have attracted more attention than any other material group with their extraordinary properties [167]. Although a lot of studies have been done, these alloys have taken their place in the world of science after the research conducted by Yeh et al. [168]. Although HEAs are different from other alloys in terms of production methods and compositions, their high strength, hardness, good corrosion resistance, excellent magnetic properties, high wear resistance, fatigue resistance, and toughness make these alloys much superior and different from other traditional alloys [61, 168–170].

Figure 11 shows the four core effects of HEA such as high entropy effect, slow diffusion effect, lattice distortion, and slow mixing effect [61, 164, 171]. The structural diversity and uniqueness as observed with HEAs are mainly due to their metastability. Such diversity in HEAs primarily arises from the lattice distortions due to the interactions between atomic size misfits and chemical disorder. Lattice distortion is the key contributor for the strengthening of the alloy and its ductility. The slow diffusion process during the formation of HEAs also enables them to maintain stability at high temperatures [172]. In HEAs, simple structured BCC, FCC, or FCC with BCC phases can be formed easily due to the high entropy mixing effect. When suitable conditions are provided, HEAs can be formed from simple solid solution phases as well as amorphous, amorphous with nanocrystalline phases. In this respect, it is worth reminding about the three basic parameters as enunciated in the Hume-Rothery rules on the solid solutions such as the atomic size difference, electronegativity, and electron concentration to predict the phases that may occur in HEAs. Hume-Rothery rules basically delineate the dissolution conditions of an element in a metal to form a solid solution, which can be either substitutional solid solutions or interstitial solid solutions. This concept is used to understand multi-component alloys such as HEA [173]. Apart from these rules, there are also parameters such as ΔH_{mix} and ΔS_{mix} that affect the design of HEAs. In a thermodynamic system, the Gibbs free energy (G) tends to be minimized under isobaric and isothermal conditions. This orientation is known as the tendency to equilibrate the system, and equilibrium conditions are met when the G value is minimal. The free energy of a system can be expressed thermodynamically using the following equation.

$$G = H - TS \tag{3}$$

where H is the enthalpy, S is the entropy, and T is the temperature. From this equation, it is clear that the enthalpy of the mixture and the entropy of the mixture directly affect the equilibrium state. Thermodynamic calculations of elemental mixtures are made using the following equation.

$$\Delta G_{mix} = \Delta H_{mix} - T\Delta S_{mix} \tag{4}$$

According to the Boltzman hypothesis, the entropy of a resultant alloy of equal atomic structure is calculated by the following equation.

$$\Delta S_{mix} = R \ln (n) \tag{5}$$

where R is the gas constant and it corresponds to a value of 8.31 J/K mol. The mixing entropies of HEAs containing 5 elements and 8 elements were calculated as 1.61 R and 2.08 R, respectively, using Eq. 3. It has been suggested by Yeh et al. to combine at least five elements in an equal or near-equal ratio for HEA. Because, for the formation of simple solid solution phases, the lowest element number for which the entropy of the mixture balances the enthalpy of the mixture was found to be 5. The mixing entropy value increases up to the addition of 13 constituent elements in an HEA. However, for any further addition beyond 13 elements, the increase in the entropy value becomes negligible.

A complete solubility of an element into another element can occur when the difference (δ) in atomic sizes between the elements is less than 15% (δ< 15%). The phase structures corresponding to ΔH_{mix} and δ values are shown in Fig. 12. It is seen that the solid solutions are formed when $\delta \leq 6.6$ and mixing enthalpy is in the range of $-11.6 < \Delta H_{mix} < 3.2$ kJ/mol. On the other hand, the values of $\delta > 6.4$ and $\Delta H_{mix} < 12.2$kJ/mol correspond to the formation of amorphous phases. The alloys to be synthesized can be predicted by interpreting the values obtained from the theoretical calculations or experimental results obtained after MA process [172, 173].

The reasons why HEAs are interesting since they contain more than one superior properties which are otherwise difficult to obtain in other material groups in a single alloy form. Fabrication of these alloys can easily be carried out in very high purity forms using MA [163, 164, 166]. HEAs comprising ferrous alloys have become the materials of great interest because of their good soft magnetic properties. Studies have shown that approximately 9% of the electricity produced is lost due to the core losses in transformers. It is known that even small changes in the magnetic properties used in transformer cores can affect energy efficiency and the cost significantly. The biggest limitations of conventional magnetic core materials are the inferior material strength and poor

Table 5 Soft magnetic HEAs synthesized by MA

Alloy composition		M_s (emu/g)	H_c (Oe)	Form	Ref.
$Co_{35}Cr_5Fe_{20}Ni_{20}Ti_{20}$					
milled for 10 h		45.9	16.5		
Heated up to 200 C for 2 h		78.8	20.2	HEA	[180]
Heated up to 200 C for 10 h		80.6	15.9		
Heated up to 700 C for 2h		86.8	98.6		
FeCoNiAlCrx					
X=	0.1	89.8	57.9		[182]
	0.3	86.2	76.7	HEA	
	0.5	80.5	77.0		
	0.7	82.7	61.2		
	0.9	74.9	58.8		
FeCoNiCuZn milled for 12 h		65.9	25	HEA	[181]
Co_xCrCuFeMnNi milled for 50 h					
x=	0.5	21	63		
	1.0	32	27		
	1.5	40	19	HEA	[8]
	2.0	52	14		
CoCuFeMnNi milled for (50 h)		84	6	HEA	[179]
$CoCr_{0.5}$CuFeMnNi milled for (50 h)		61	8		
$CoCr_{1.0}$CuFeMnNi milled for (50 h)		33	26	HEA	[179]
$CoCr_{1.5}$CuFeMnNi milled for (50 h)		24	67		
CoCrFeNi milled for 200 h		13.9	15.7	HEA	[183]
FeSiBAlNiNb					
milled for	40 h	30	280		
	100 h	11	350	HEA	[184]
	260 h	3	270		
TiC/$Fe_{30}Ni_{30}Co_{29}Cu_{5.5}Mn_{5.5}$ milled for 40 h		107.2	3.3	HEA	[185]
$Co_{35}Cr_5Fe_{20}Ni_{20}Ti_{20}$					
milled for 20 h		46	15	HEA	[186]
milled for 20 h and annealed at 200 C		81	15		
TiFeNiCrCo milled for 10 h		24.4	149.5	HEA	[187]
FeCoNi($B_{0.5}Si_{0.5}$)					
milled for 150 h		94.3	49.0		
Annealed at 650 C		127.3	29.5	HEA	[188]
MA +SPS at 750 C		110.9	25.0		
MA+SPS at 1000 C		115.8	27.9		
AlCoCrFeNi (milled for 30h)		47.7	121.2	HEA	[178]
Sintered at 1173 K		70.0	51.4		
FeNiCoCrNb milled for 20 h		20.9	81	HEA	[189]
AlCoCrFeNiTiZn					
milled for 120 h		40.36	114.84	HEA	[190]
$Co_{35}Cr_5Fe_{10}Ni_{30}Ti_{20}$					
milled for 20 h		74.8	12.92	HEA	[191]
$Fe_{50}Ni_{10}Co_{10}Ti_{10}B_{20}$					
milled for 50 h			89.7	32	
heat treated at 300 C			101.9	13.3 HEA	[192]
Heat treated					
heat treated at 700 C			38.3	72.2	
FeSiBAlNi					
milled for 160 h			30	75–85 HEA	[193]

ductility to overcome such deficiencies of the conventional transformers, and it is now more of a challenge to develop a new generation material with superior soft magnetic properties. The major requirements for the new generation magnetic materials are to have high M_s, low H_c, high electrical resistance (to decrease eddy current loss), and above all a good compromise to maintain a balance on the material strength and on the magnetic properties [174, 175]. The excellent mechanical and magnetic properties of HEAs make them the materials of great attention in the scientific world. These fundamental characteristics of HEAs enable them to be used in transformer cores, electromagnetic magnets, magnetic recording devices, and high-performance smart devices especially in the high usage areas of soft magnetic materials. The need for improved soft magnetic materials of superior magnetic properties has been leading the search for novel materials in perpetuity [176, 177]. As a result, HEAs have become the materials of choice for exploration. HEAs can be synthesized by using various methods, of which MA happens to be the most convenient one due to its advantageous features over the other methods as discussed above and elsewhere [14]. Using the MA method, nanocrystals, high entropy alloys, intermetallic, amorphous materials, nanocomposites, and even amorphous + nanocrystal structures can be synthesized in a single alloy. Furthermore, it is relatively less costly and suitable for the mass production when compared to other methods of synthesis. Vikas et al successfully synthesized AlCoCrFeNi HEA alloy by milling for 30 h by MA using a planetary type of ball-mill. After 30-h alloying and then followed by 2-h sintering at 1173 K, the M_s of the alloy was found to increase from 47.7 to 70 emu/g with a significant drop in H_c from 121.2 to 51.4 Oe. It is clear that the sintering process has a great influence on the magnetic properties to obtain higher M_s with soft magnetic properties [178]. In another study, $CoCr_xCuFeMnNi$ (x = 0, 0.5, 1.0, 1.5, 2.0 mol) was synthesized as supersaturated solid solutions in a planetary type of mill by Zhao et al. Samples were first dry-milled for 45 h followed by wet milling for 5 h by adding ethanol. M_s and H_c values of the alloys formed with Cr at 0, 0.5, 1.0, 1.5, and 2.0 mol additions were examined by Zhao et al. It showed a decrease in M_s and an increase in H_c as the level of Cr increased in the alloy [179]. Table 5 summarizes the magnetic features of the HEAs recently synthesized by MA demonstrating their efficacies as candidates for soft magnetic materials.

5 Conclusions

This review provides an overview of soft magnetic materials, as well as the soft magnetic properties of amorphous/nanocrystalline alloys and HEAs particularly synthesized by the MA method, and also the effect of annealing on their properties.

- The effect of parameters used in the MA method on soft magnetic properties of amorphous/nanocrystal alloys was investigated. As a summary, as the milling time increases, phase transformations are observed in the alloys and consequently, significant changes occur in the mechanical and magnetic properties. These changes differ depending on the alloy compositions and milling conditions. As a result of investigation, it was found that when the appropriate milling time and conditions are selected, the MA could improve the soft magnetic properties of the alloy. On the other hand, as the milling time increases, dislocations occur which cause micro-strains. This situation negatively affects the magnetic properties, but this challenge can be overcome by the appropriate annealing process.
- When the alloys formed by MA are annealed at certain temperatures over a certain time period, their soft magnetic properties significantly improve. For example, the M_s of the FeCoNiCuAl alloy after the MA process is 73 emu/g where it is successfully increased to 94.2 emu/g after a suitable annealing process. The annealing causes phase transformations by removing the stresses in the microstructure and provides the improvement of the soft magnetic properties. Researches show that the annealing at the appropriate temperature and time improves not only the soft magnetic but also the mechanical properties.
- On the other hand, it has been investigated that the addition of PCA enables phase transformations, formation of amorphous structure, development of glass-forming capability, shortening of alloying time, and control of chemical reactions. It was observed that the soft magnetic properties of the alloys improved when a suitable PCA was applied during milling.
- The material groups such as amorphous/nanocrystalline alloys and HEA having soft magnetic properties are used in almost every field where electricity and electronics involved, from military to health, from electronic devices to electricity distribution facilities.
- As a result, it has been observed that especially nanocrystal/amorphous alloys have better and more interesting properties than traditional soft magnetic materials and are promising for soft magnetic applications.
- Additionally, despite HEAs rather being the recent developments compared to the other magnetic materials, they gained considerable attention due to their superior mechanical as well as soft magnetic properties. The investigation carried out in this review shows that HEAs can be the very formidable alternative for soft magnetic applications.

Declarations

Conflict of interest The authors declare no competing interests.

References

1. F. Fiorillo, G. Bertotti, C. Appino, M. Pasquale, *Wiley Encyclopaedia of Electrical and Electronics Engineering* (2016). https://doi.org/10.1002/047134608X
2. B.D. Cullity, C.D. Graham, *Introduction to Magnetic Materials*, 2nd edn. (IEEE Press, Piscataway, New Jersey, 2009)
3. M.H. Khazaei Feizabad, E. Sarvestani, G.R. Khayati, J. Alloys Compd. (2020). https://doi.org/10.1016/j.jallcom.2020.155646
4. U. Patil, S.-J. Hong, C. Suryanarayana, J. Alloys Compd. (2005). https://doi.org/10.1016/j.jallcom.2004.08.020
5. P. Duwez, S.C.H. Lin, J. Appl. Phys. (1967). https://doi.org/10.1063/1.1709084
6. Y. Yoshizawa, S. Oguma, K. Yamauchi, J. Appl. Phys. (1988). https://doi.org/10.1063/1.342149
7. C. Suryanarayana, Research (2019). https://doi.org/10.34133/2019/4219812
8. N. Metidji, N.E. Bacha, A. Younes, D. Saidi, Powder Metall. Met. C. (2020). https://doi.org/10.1007/s11106-020-00148-3
9. A. Inoue, F. Kong, *Encyclopedia of Smart Materials* (2020). https://doi.org/10.1016/B978-0-12-803581-8.11725-4
10. N.S. Kumar, R.P. Suvarna, K.C.B. Naidu, M.S.S.R.K.N. Sarma, R. Pothu, R. Boddula, in *Alloy Materials and Their Allied Applications*, ed. by Inamuddin, R. Boddula, M. I. Ahamed, A. M. Asiri. (© 2020 Scrivener Publishing LLC, 2020), pp. 73–90
11. W. Gao, Y. Dong, X. Jia, L. Yang, X. Li, S. Wu, R. Zhao et al., Novel CoFeAlMn high-entropy alloys with excellent soft magnetic properties and high thermal stability. J. Mater. Sci. Technol. (2023). https://doi.org/10.1016/j.jmst.2023.01.010
12. J.M. Coey, *Magnetism and magnetic materials* (Cambridge university press, New York, 2010), p. 596
13. D. Jiles, *Introduction to Magnetism and Magnetic Materials* (Ames, Department of Materials Science and Engineering, Iowa State University, 1990), p. 454
14. C. Suryanarayana, *Mechanical alloying and milling* (Pmatsci, 2001), pp. 1–184
15. C. Suryanarayana, Recent developments in mechanical alloying. Rev. Adv. Mater. Sci., 203–211 (1996)
16. T. Şimşek, J. Boron (2019). https://doi.org/10.30728/boron.500470
17. B. Avar, S. Ozcan, J. Alloys Compd. (2015). https://doi.org/10.1016/j.jallcom.2015.07.268
18. R. Koohkan, S. Sharafi, H. Shokrollahi, K. Janghorban, J. Magn. Magn. Mater. (2008). https://doi.org/10.1016/j.jmmm.2007.10.033
19. M.H. Enayati, F.A. Mohamed, Int. Mater. Rev. (2014). https://doi.org/10.1179/1743280414Y.0000000036
20. F.C. Li, T. Liu, J.Y. Zhang, S. Shuang, Q. Wang, A.D. Wang, J.G. Wang, Y. Yang, Mtadv (2019). https://doi.org/10.1016/j.mtadv.2019.100027
21. F. Popa, O. Isnard, I. Chicinas, V. Pop, J. Alloys Compd. (2013). https://doi.org/10.1016/j.jallcom.2012.11.164
22. W. Klement Jr., R.H. Wıllens, P. Duwez, Nature **187**(1960), 869–870 (1960)
23. P. Duwez, R.H. Wıllens, R.C. Crewdson, J. Appl. Phys. (1965). https://doi.org/10.1063/1.1714461
24. A. Inoue, A. Takeuchi, Acta Mater. (2011). https://doi.org/10.1016/j.actamat.2010.11.027
25. R. Alben, J. Becker, M. Chi, J. Appl. Phys. (1978). https://doi.org/10.1063/1.324881
26. G. Herzer, IEEE Trans. Magn. (1989). https://doi.org/10.1109/20.42292
27. E. Vafaeı-Makhsoos, E.L. Thomas, L.E. Toth, Metall. Trans. A. (1978). https://doi.org/10.1007/BF02661817
28. Advanced Interior Materials; Global Soft Magnetic Material Market Size Report, 2020-2027; Report ID: GVR-4-68038-932-6, Pages 120
29. R. Hasegawa, D. Azuma, J. Magn. Magn. Mater. (2008). https://doi.org/10.1016/j.jmmm.2008.04.052
30. H.R. Lashgari, D. Chu, S. Xie, H. Sun, M. Ferry, S. Li, A review study. J. Non-Cryst. Solids (2014). https://doi.org/10.1016/j.jnoncrysol.2014.03.010
31. G. Herzer, IEEE Trans. Magn. (1990). https://doi.org/10.1109/20.104389
32. R. Alben, J.J. Becker, M.C. Chi, J. Appl. Phys. (1978). https://doi.org/10.1063/1.324881
33. H. Kronmüller, S. S. P. Parkin (eds.), *Handbook of Magnetism and Advanced Magnetic Materials*, vol 2 (Wiley, New York, 2007)
34. J. Becker, F. Luborsky, J.W. Walter, Magnetic moments and Curie temperatures of (Fe, Ni) 80 (P, B) 20 amorphous alloys. IEEE Trans. Magn. **1977** (1977). https://doi.org/10.1109/TMAG.1977.1059499
35. R.C. O'Handley, R. Hasegawa, R. Ray, C.P. Chou, Appl. Phys. Lett. (1976). https://doi.org/10.1063/1.89085
36. F.L. Kong, C.T. Chang, A. Inoue, E. Shalaan, F. Al-Marzouki, J. Alloys Compd. (2014). https://doi.org/10.1016/j.jallcom.2014.06.093
37. F. Wang, A. Inoue, Y. Han, S.L. Zhu, F.L. Kong, E. Zanaeva, G.D. Liu, E. Shalaan, F. Al-Marzouki, A. Obaid, J. Alloys Compd. (2017). https://doi.org/10.1016/j.jallcom.2017.06.192
38. J. Xu, X. Liu, Y. Wang, Q. Shi, J. Wang, K. Li, Y. Yang, J. Alloys Compd. (2022). https://doi.org/10.1016/j.jallcom.2022.163887
39. G. Herzer, IEEE Trans. Magn. (1990). https://doi.org/10.1109/20.104389
40. K. Suzuki, A. Makino, N. Kataoka, A. Inoue, T. Masumoto, Matertrans. (1991). https://doi.org/10.2320/matertrans1989.32.93
41. N.K. Prasad, V. Kumar, J. Mater. Sci.-Mater. El. (2015). https://doi.org/10.1007/s10854-016-5090-4
42. P.S. Gilman, J.S. Benjamin, Rev. Mater. Sci. (1983). https://doi.org/10.1146/annurev.ms.13.080183.001431
43. B.S. Murty, Bull. Mater. Sci. (1993). https://doi.org/10.1007/BF02745302
44. K. Uenishi, K.F. Kobayashi, K.N. Ishihara, P.M. Shingu, Mater. Sci. Eng. (1991). https://doi.org/10.1016/0921-5093(91)90987-X
45. H.J. Fecht, G. Han, Z. Fu, W.L. Johnson, J. Appl. Phys. (1990). https://doi.org/10.1063/1.345624
46. J. Eckert, L. Schultz, K. Urban, Mater. Sci. Eng. (1991). https://doi.org/10.1016/0921-5093(91)90095-5
47. C.C. Koch, Annu. Rev. Mater. Sci. (1989). https://doi.org/10.1146/annurev.ms.19.080189.001005
48. M. Oehring, R. Bormann, Mater. Sci. Eng. (1991). https://doi.org/10.1016/0921-5093(91)90984-U
49. G. Wang, M. Liu, L. Wang, H. Liu, Mater. Express (2019). https://doi.org/10.1166/mex.2019.1541
50. K.F. Ulbrich, C.E.M. Campos, J. Magn. Magn. Mater. (2020). https://doi.org/10.1016/j.jmmm.2019.165706
51. T.F. Marinca, A.I. Sule, R. Hirian, A.N. Sechel, F. Popa, B.V. Neamțu, I. Chicinaș, Adv. Powder Technol. (2022). https://doi.org/10.1016/j.apt.2022.103642

52. T.F. Marinca, I. Chicinas, O. Isnard, V. Popescu, J. Am. Ceram. Soc. (2013). https://doi.org/10.1111/jace.12043
53. S. Rezgoun, E. Sakher, S. Chouf, M. Bououdina, M. Benchiheub, S. Bellucci, J. Supercond. Nov. Magn. (2020). https://doi.org/10.1007/s10948-020-05455-9
54. A.M. Padhan, B. Kisan, P. Alagarsamy, J. Magn. Magn. Mater. (2020). https://doi.org/10.1016/j.jmmm.2019.165784
55. C.-V. Prica, T.F. Marinca, F. Popa, N.A. Sechel, O. Isnard, I. Chicinas, Adv. Powder Technol. (2016). https://doi.org/10.1016/j.apt.2016.01.018
56. M. Pekala, M. Jachimowicz, V.I. Fadeeva, H. Matyja, J. Non-Cryst. Solids (2001). https://doi.org/10.1016/S0022-3093(01)00602-0
57. L.M. Moreno, J.S. Blázquez, J.J. Ipus, J.M. Borrego, V. Franco, A. Conde, J. Appl. Phys. (2014). https://doi.org/10.1063/1.4857595
58. A.I. Gusev, Phys.-Usp. (2020). https://doi.org/10.3367/UFNe.2019.06.038581
59. L.G. Betancourt-Cantera, F. Sanchez-De Jesus, A.M. Bolarín-Miro, A. Gallegos-Melgar, J. Mayen, J.A. Betancourt-Cantera, J. Mater. Res. Technol. (2020). https://doi.org/10.1016/j.jmrt.2020.10.068
60. M. Ali, F. Ahmad, Mater. Manuf. Process. (2020). https://doi.org/10.1080/10426914.2019.1662038
61. Z. Zhang, B. Luo, H. Zhou, F. Wang, MSF. (2020). https://doi.org/10.4028/www.scientific.net/msf.993.806
62. S. Abbasi, H. Eslamizadeh, H. Raanaei, J. Magn. Magn. Mater. (2018). https://doi.org/10.1016/j.jmmm.2017.12.015
63. I. Ismail, M. Hashim, K.A. Matori, R. Alias, J. Hassan, J. Magn. Magn. Mater. (2011). https://doi.org/10.1016/j.jmmm.2011.01.002
64. G. Bertotti, J. Magn. Magn. Mater. (2008). https://doi.org/10.1016/j.jmmm.2008.04.001
65. F. Alijani, M. Reihanian, K. Gheisari, J. Alloys Compd. (2018). https://doi.org/10.1016/j.jallcom.2018.09.204
66. N. Rabie, G.R. Gordani, A. Ghasemi, J. Magn. Magn. Mater. (2017). https://doi.org/10.1016/j.jmmm.2017.03.063
67. R.-F. Zhao, B. Ren, G.-P. Zhang, Z.-X. Liu, J.-j. Zhang, J. Magn. Magn. Mater. (2018). https://doi.org/10.1016/j.jmmm.2018.07.072
68. Y. Duan, Y. Cui, B. Zhang, G. Ma, W. Tongmin, J. Alloys Compd. (2019). https://doi.org/10.1016/j.jallcom.2018.09.096
69. H. Raanaei, V. Mohammad-Hosseini, J. Magn. Magn. Mater.. https://doi.org/10.1016/j.jmmm.2016.04.040
70. H. Shokrollahi, Mater. Des. (2009). https://doi.org/10.1016/j.matdes.2009.03.035
71. D. Yuting, M. Guofeng, IOP Conf. Ser.: Earth Environ. Sci. (2020). https://doi.org/10.1088/1755-1315/565/1/012048
72. D. Azuma, N. Itoa, M. Ohta, J. Magn. Magn. Mater. (2020). https://doi.org/10.1016/j.jmmm.2019.166373
73. A. Kumar, A. Singh, A. Suhane, J. Mater. Sci. Technol. (2022). https://doi.org/10.1016/j.jmrt.2022.01.141
74. D. Azuma, in *In Wide Bandgap Power Semiconductor Packaging*. Magnetic materials (Woodhead Publishing, 2018), pp. 97–107
75. J. Fuzer, J. Bednarcık, P. Kollar, S. Roth, J. Magn. Magn. Mater. (2007). https://doi.org/10.1016/j.jmmm.2007.03.112
76. C. Suryanarayana, Mater. Today (2012). https://doi.org/10.1016/S1369-7021(12)70218-3
77. Q. Zeng, I. Baker, V. McCreary, Z. Yan, J. Magn. Magn. Mater. (2007). https://doi.org/10.1016/j.jmmm.2007.04.037
78. M.H.K. Feizabad, S. Sharafi, G. Reza Khayati, M. Ranjbar, J. Magn. Magn. Mater. (2017). https://doi.org/10.1016/j.jmmm.2017.10.018
79. A.H. Taghvaei, F. Ghajari, D. Markó, K.G. Prashanth, J. Magn. Magn. Mater. (2015). https://doi.org/10.1016/j.jmmm.2015.07.073
80. T.D. Shen, R.B. Schwarz, J.D. Thompson, Phys. Rev. (2005). https://doi.org/10.1103/PhysRevB.72.014431
81. G.V. Thotakura, A. Rathi, T.V. Jayarama, Appl. Phys. A Mater. Sci. Process. (2019). https://doi.org/10.1007/s00339-019-2535-7
82. H. Raanaei, M. Rahimi, V. Mohammad-Hosseini, J. Magn. Magn. Mater. (2020). https://doi.org/10.1016/j.jmmm.2020.166870
83. H. Yaykasli, B. Avar, M. Panigrahi, M. Gogebakan, H. Eskalen, Arab. J. Sci. Eng. (2022). https://doi.org/10.1007/s13369-022-07037-4
84. A. Carrillo, L. Escoda, J. Saurina, J.J. Suno, AIP Adv. (2018). https://doi.org/10.1063/1.4994144
85. E.B. Yekta, M. Adineh, H. Nasiri, H. Shalchian, J. Alloys Compd. (2018). https://doi.org/10.1016/j.jallcom.2018.09.188
86. A.H. Taghvaei, M. Stoica, M.S. Khoshkhoo, J. Thomas, G. Vaughan, K. Janghorban, J. Eckert, Mater. Chem. Phys. (2012). https://doi.org/10.1016/j.matchemphys.2012.04.031
87. B. Avar, A.K. Chattopadhyay, T. Simsek et al., Synthesis and characterization of amorphous-nanocrystalline $Fe_{70}Cr_{10}Nb_{10}B_{10}$ powders by mechanical alloying. Appl. Phys. A **128**, 537 (2022). https://doi.org/10.1007/s00339-022-05680-0
88. T. Şimşek, Boron (2019). https://doi.org/10.30728/boron.500470
89. K. Gheisari, S. Javadpour, J. Magn. Magn. Mater. (2013). https://doi.org/10.1016/j.jmmm.2013.05.007
90. A. Younes, N. Dilmi, M.M. Khorchef, A. Bouamer, N.-E. Bacha, M. Zergoug, Appl. Surf. Sci. (2017). https://doi.org/10.1016/j.apsusc.2017.12.160
91. R. Hamzaoui, O. Elkedim, N. Fenineche, E. Gaffet, J. Craven, Mater. Sci. Eng. (2003). https://doi.org/10.1016/S0921-5093(03)00460-X
92. H. Ibn, T. Gharsallah, J. Makhlouf, L. Saurina, J.J. Escoda, N. Suñol, M.K. Llorca-Isern, Mater. Lett. (2016). https://doi.org/10.1016/j.matlet.2016.05.190
93. T. Clark, S.N. Mathaudhu, J. Magn. Magn. Mater. (2019). https://doi.org/10.1016/j.jmmm.2019.03.070
94. A. Behvandi, H. Shokrollahi, B. Chitsazan, M. Ghaffari, J. Magn. Magn. Mater. (2010). https://doi.org/10.1016/j.jmmm.2010.08.025
95. M.A. Nowroozi, H. Shokrollahi, J. Magn. Magn. Mater. (2013). https://doi.org/10.1016/j.jmmm.2013.01.034
96. E.B. Yekta, A.H. Taghvaei, S. Shahriar, Powder Technol. (2017). https://doi.org/10.1016/j.powtec.2017.08.059
97. M. Hocine, A. Guittoum, M. Hemmous, D. Martínez-Blanco, P. Gorria, B. Rahal, J.A. Blanco, J.J. Sunol, A. Laggoun, J. Magn. Magn. Mater. (2016). https://doi.org/10.1016/j.jmmm.2016.08.058
98. M. Mohammadi, A. Ghasemi, M. Tavoosi, J. Magn. Magn. Mater.. https://doi.org/10.1016/j.jmmm.2016.06.037
99. M. Imani, M.H. Enayati, A.K. Basak, Mater. Express. https://doi.org/10.1088/2053-1591/ab167d
100. A.A. Abouchenari, M. Moradi, JCC (2019). https://doi.org/10.29252/jcc.1.1.2
101. A. Azizi, H. Yoozbashizadeh, S.K. Sadrnezhaad, J. Magn. Magn. Mater., 2729–2732 (2009). https://doi.org/10.1016/j.jmmm.2009.03.085
102. L. Wei, L. Yang, B. Yan, W.-h. Huang, L. Bin, J. Alloys Compd. (2006). https://doi.org/10.1016/j.jallcom.2005.06.059
103. Z. Bensebaa, B. Bouzabata, A. Otmani, A. Djekoun, A. Kihal, J.M. Greneche, J. Magn. Magn. Mater. (2010). https://doi.org/10.1016/j.jmmm.2010.01.040
104. M. Khajepour, S. Sharafi, J. Alloys Compd. (2011). https://doi.org/10.1016/j.jallcom.2011.04.095
105. M. Yousefi, S. Sharafi, A. Mehrolhosseiny, Adv. Powder Technol. (2014). https://doi.org/10.1016/j.apt.2013.11.008
106. M.P.C. Kalita, A. Perumal, A. Srinivasan, J. Magn. Magn. Mater. (2008). https://doi.org/10.1016/j.jmmm.2008.06.014

107. R. Hamzaoui, O. Elkedim, E. Gaffet, Mater. Sci. Eng. A Struct. Mater. (2004). https://doi.org/10.1016/j.msea.2004.05.008
108. J. Ding, Y. Shi, L.F. Chen, C.R. Deng, S.H. Fuha, Y. Li, J. Magn. Magn. Mater. (2002). https://doi.org/10.1016/S0304-8853(02)00173-7
109. E. Ghasemi, A. Ghasemi, M. Hadi, M. Sadeghi, S.H. Hashemi, M. Tavoosi, G.R. Gordani, J. Magn. Magn. Mater. (2018). https://doi.org/10.1016/j.jmmm.2018.07.062
110. N. Khitouni, R. Daly, L. Escoda, N. Llorca-Isern, J.J. Suñol, M. Dammak, M. Khitouni, J. Supercond. Nov. Magn. (2020). https://doi.org/10.1007/s10948-020-05500-7
111. A. Abuchenari, F. Sharifianjazi, C. Amirhosein Pakseresht, M.P.A. Esmaeilkhanian, Adv. Powder Technol. (2021). https://doi.org/10.1016/j.apt.2020.12.011
112. M. Hemmous, A. Guittoum, M. Kezrane, N. Boukherroub, D. Martínez-Blanco, P. Gorria, J.A. Blanco, N. Souami, N. Fenineche, J. Magn. Magn. Mater. (2017). https://doi.org/10.1016/j.jmmm.2017.05.010
113. K. Bazzi, V.M. Meka, A. Rathi, T.V. Jayaraman, Mater. Chem. Phys. (2019). https://doi.org/10.1016/j.matchemphys.2019.01.044
114. J. Sravani, S.V. Kummari, A. Dhole, V.V.S.S. Srikanth, C. Bansal, A. Rajanikanth, Mater. Lett. (2019). https://doi.org/10.1016/j.matlet.2019.126576
115. A.F. Manchón-Gordón, J.J. Ipus, J.S. Blázquez, C.F. Conde, A. Conde, P. Svec Sr., J. Alloys Compd. (2020). https://doi.org/10.3390/ma13020490
116. P. Ramasamy, R.N. Shahid, S. Scudino, J. Eckert, M. Stoica, J. Alloys Compd. (2017). https://doi.org/10.1016/j.jallcom.2017.07.160
117. A. Rathi, T.V. Jayaraman, Met. Mater. Ser. (2018). https://doi.org/10.1007/978-3-030-05749-7_14
118. E.B. Yekta, A.H. Taghvaei, S. Sharafi, J. Non-Cryst. Solids (2018). https://doi.org/10.1016/j.jnoncrysol.2018.06.040
119. C.D. Stanciu, J.B. Marimon da Cunha, I. Chicinas, O. Isnard, J. Alloys Compd. (2019). https://doi.org/10.1016/j.jallcom.2019.05.156
120. Y. Ma, X. Yin, B. Shao, Q. Yang, Q. Shen, X. Zhou, J. Sun, D. Guo, K. Li, J. Mater. Sci. (2019). https://doi.org/10.1007/s10853-018-2989-6
121. K. Brzózkaa, T. Szumiataa, D. Olekšákováb, P. Kollár, Acta Phys. Pol. A (2020). https://doi.org/10.12693/APhysPolA.137.726
122. Y. Han, Z. Wang, X. Yan-chao, Z.-y. Xie, L.-j. Li, J. Non-Cryst. Solids (2016). https://doi.org/10.1016/j.jnoncrysol.2016.04.003
123. S.B. Dalavi, J. Theerthagiri, M. Manivel Raja, R.N. Panda, J. Magn. Magn. Mater. (2013). https://doi.org/10.1016/j.jmmm.2013.05.026
124. Y. Srivastava, S. Srivastava, J. Magn. Magn. Mater. (2017). https://doi.org/10.1016/j.jmmm.2016.07.067
125. H. Raanaei, V. Mohammad-Hosseini, J. Magn. Magn. Mater. (2016). https://doi.org/10.1016/j.jmmm.2016.04.040
126. C.-H. Lee, J. Nanosci. Nanotechnol. (2018). https://doi.org/10.1166/jnn.2018.14923
127. M. Barıs, T. Sımsek, A. Akkurt, Bull. Mater. Sci. (2016). https://doi.org/10.1007/s12034-016-1231-x
128. B.V. Neamtu, T.F. Marinca, I. Chicinas, O. Isnard, F. Popa, Adv. Powder Technol. (2014). https://doi.org/10.1016/j.apt.2014.10.014
129. B. Avar, *Nanokristal Co70Si15B15 Süleyman Demirel Üniversitesi Fen Bilimleri Enstitüsü Dergisi* (2019). https://doi.org/10.19113/sdufenbed.447300
130. H. Ahmadian Baghbaderani, S. Sharafi, M.D. Chermahini, Powder Technol. (2012). https://doi.org/10.1016/j.powtec.2012.07.039
131. B.V. Neamţu, H.F. Chicinaş, T.F. Marinca, O. Isnard, I. Chicinaş, J. Alloys Compd. (2016). https://doi.org/10.1016/j.jallcom.2016.02.233
132. H. Raanaei, M. Fakhraee, J. Magn. Magn. Mater. (2017). https://doi.org/10.1016/j.jmmm.2017.04.080
133. M.S. El-Eskandarany, N. Ali, M. Saeed, Nanomaterials (2020). https://doi.org/10.3390/nano10050849
134. M.S. El-Eskandarany, S. Ishihara, W. Zhang, A. Inoue, Metall. Mater. Trans. A (2005). https://doi.org/10.1007/s11661-005-0146-8
135. H. Raanaeia, M. Rahimi, V. Mohammad-Hosseini, J. Magn. Magn. Mater. (2020). https://doi.org/10.1016/j.jmmm.2020.166870
136. H.S. Nickjeh, A.H. Taghvaei, P. Ramasamy, J. Eckert, J. Alloys Compd. **155913** (2020). https://doi.org/10.1016/j.jallcom.2020.155913
137. M.S. El-Eskandarany, N. Ali, Molecules **25**(3338) (2020). https://doi.org/10.3390/molecules25153338
138. C. Li, H.R.D. Chen, K. Li, D.G.B. Shao, Microsc. Res. Tech. (2018). https://doi.org/10.1002/jemt.23038
139. M. Triki, H. Mechri, H. Azzaz, M. Azzaz, J. Magn. Magn. Mater. (2022). https://doi.org/10.1016/j.jmmm.2021.168514
140. A. Hajalilou, S.A. Mazlan, Appl. Phys. A Mater. Sci. Process. (2016). https://doi.org/10.1007/s00339-016-0217-2
141. R. Hassan, J. Hassan, M. Hashim, S. Paiman, R.'a.S. AZIS, J. Adv. Ceram. (2014). https://doi.org/10.1007/s40145-014-0122-0
142. I.R. Ibrahim, M. Hashim, R. Nazlan, I. Ismail, W.N.W.A. Rahman, N.H. Abdullah, F.M. Idris, M.S.E. Shafie, M.M.M. Zulkimi, J. Magn. Magn. Mater. (2014). https://doi.org/10.1016/j.jmmm.2013.12.024
143. A. Hajalilou, A. Kianvash, H. Lavvafi, K. Shameli, a review. J. Mater. Sci.-Mater. El (2017). https://doi.org/10.1007/s10854-017-8082-0
144. R. Parsons, Z. Li, K. Suzuki, J. Magn. Magn. Mater. (2019). https://doi.org/10.1016/j.jmmm.2019.04.052
145. V. Sepelak, D. Baabe, D. Mienert, D. Schultzec, F. Krumeich, F.J. Litterst, K.D. Becker, J. Magn. Magn. Mater. (2003). https://doi.org/10.1016/S0304-8853(02)01279-9
146. R. Besmel, M. Ghaffari, H. Shokrollahi, B. Chitsazan, L. Karimi, J. Magn. Magn. Mater. (2011). https://doi.org/10.1016/j.jmmm.2011.05.025
147. T. Ashokkumar, A. Rajadurai, Gouthama, S.C.B. Gopinath, J. Magn. Magn. Mater. (2018). https://doi.org/10.1016/j.jmmm.2018.06.008
148. A. Ghasemi, K. Zamani, M. Tavoosi, G.R. Gordan, J. Supercond. Nov. Magn. (2020). https://doi.org/10.1007/s10948-020-05579-y
149. S. Zahi, M. Hashim, A.R. Daud, J. Magn. Magn. Mater. (2007). https://doi.org/10.1016/j.jmmm.2006.05.033
150. N. Loudjani, T. Gouasmia, M. Bououdina, J.L. Bobet, J. Alloys Compd. (2020). https://doi.org/10.1016/j.jallcom.2020.156392
151. S. Souilah, S. Alleg, M. Bououdina, J.J. Sunol, E.K. Hlil, J. Supercond. Nov. Magn. (2017). https://doi.org/10.1007/s10948-017-4001-0
152. S.W. Du, R.V. Ramanujan, J. Magn. Magn. Mater. (2005). https://doi.org/10.1016/j.jmmm.2004.11.143
153. V. Sepelak, I. Bergmann, A. Feldhoff, P. Heitjans, F. Krumeich, D. Menzel, F.J. Litterst, S.J. Campbell, K.D. Becker, J. Phys. Chem. C (2007). https://doi.org/10.1021/jp067620s
154. M. Jalaly, M.H. Enayati, F. Karimzadeh, P. Kameli, Powtec. (2009). https://doi.org/10.1016/j.powtec.2009.03.008
155. M. Jalaly, M.H. Enayati, F. Karimzadeh, J. Alloys Compd. (2009). https://doi.org/10.1016/j.jallcom.2009.02.042
156. T.F. Marinca, I. Chicinaş, O. Isnard, B.V. Neamţu, Ceram. Int. (2015). https://doi.org/10.1016/j.ceramint.2015.11.155
157. L. Hosseınzadeha, J. Baedıa, A.K. Zak, Bull. Mater. Sci. (2014). https://doi.org/10.1007/s12034-014-0055-9
158. C.N. Chinnasamy, A. Narayanasamy, N. Ponpandian, Phys. Rev. B Condens. Matter (2001). https://doi.org/10.1103/PhysRevB.63.184108

159. A. Guittoum, A. Layadi, A. Bourzami, H. Tafat, N. Souami, S. Boutarfaiad, D. Lacour, J. Magn. Magn. Mater. (2008). https://doi.org/10.1016/j.jmmm.2007.11.021
160. J.A. Castrillon Arango, A.A. Cristobal, C.P. Ramos, P.G. Bercoff, P.M. Botta, J. Alloys Compd. (2019). https://doi.org/10.1016/j.jallcom.2019.152044
161. A. Rathi, V.M. Meka, T.V. Jayaraman, J. Magn. Magn. Mater. (2018). https://doi.org/10.1016/j.jmmm.2018.09.002
162. A.A. Paul, A. Rathi, G.V. Thotakura, T.V. Jayaraman, Mater. Chem. Phys. (2020). https://doi.org/10.1016/j.matchemphys.2020.123897
163. P. Sahu, A.S. Bagri, M.D. Anoop, M. Kumar, V. Kumar, Silicon (2019). https://doi.org/10.1007/s12633-019-00182-w
164. B. Avar, T. Simsek, S. Ozcan, A.K. Chattopadhyay, B. Kalkan, J. Alloys Compd. (2020). https://doi.org/10.1016/j.jallcom.2020.158528
165. N.K. Prasad, V. Kumar, J. Mater. Sci. Mater. Electron. (2015). https://doi.org/10.1007/s10854-015-3695-7
166. M. Hajipour, H. Raanaei, S. Zarei, J. Magn. Magn. Mater. (2022). https://doi.org/10.1016/j.jmmm.2021.168992
167. B. Cantor, Prog. Mater. Sci. (2020). https://doi.org/10.1016/j.pmatsci.2020.100754
168. B.S. Murty, J.-W. Yeh, S. Ranganathan, P.P. Bhattacharjee, *High-entropy alloys*, 1st edn. (Elsevier, Londra: Butterworth-Heinemann, 2014), p. 355
169. L. Kush, S. Srivastava, Y. Jaiswal, R. Anant, JMEPEG (2020). https://doi.org/10.1007/s11665-020-04791-0
170. Y.F. Ye, Q. Wang, J. Lu, C.T. Liu, Y. Yang, Mater. Today (2015). https://doi.org/10.1016/j.mattod.2015.11.026
171. Şerzat Safaltın, Burak Küçükelyas, Sabahattin Gürmen, Teknik Yazı, Bursa Tekni Üniversitesi, İstanbul Teknik Üniversitesi, Metalurji Dergisi, 186 , (Aralık 2018).
172. S. Guo, H. Qiang, C. Ng, C.T. Liu, Intermetallics (2013). https://doi.org/10.1016/j.intermet.2013.05.002
173. A.D. Laura, *Combinatorial, submitted for the degree of Doctor of Philosophy* (Department of Materials Science and Engineering University of Sheffield, 2016)
174. P. Kumari, A.K. Gupta, R.K. Mishra, M.S. Ahmad, R.R. Shahi, J. Magn. Magn. Mater. (2022). https://doi.org/10.1016/j.jmmm.2022.169142
175. O. Gutfleisch, M.A. Willard, E. Brück, C.H. Chen, S.G. Sankar, J.P. Liu, Adv. Mater. (2011). https://doi.org/10.1002/adma201001002180
176. R. Zhao, Y. Kim, S.A. Chester, P. Sharma, X. Zhao, J. Mech. Phys. Solids (2019). https://doi.org/10.1016/j.jmps.2018.10.008
177. E.W. Huang, G.Y. Hung, S.Y. Lee, J. Jain, K.P. Chang, J.J. Chou, W.C. Yang, P.K. Liaw, Crystals. (2020). https://doi.org/10.3390/cryst10030200
178. V. Shivam, Y. Shadangi, J. Basu, N.K. Mukhopadhyay, J. Alloys Compd. (2020). https://doi.org/10.1016/j.jallcom.2020.154826
179. R.F. Zhao, B. Ren, G.P. Zhang, Z.X. Liu, B. Cai, J.J. Zhang, J. Magn. Magn. Mater. (2019, 2019). https://doi.org/10.1016/j.jmmm.2019.165574
180. K. Mishra Rajesh, R. Shahi, J. Alloys Compd. (2020). https://doi.org/10.1016/j.jallcom.2019.153534
181. Z. Yinzhe, C. Yudao, Q. Qingdong, L. Wei, J. Magn. Magn. Mater. (2019). https://doi.org/10.1016/j.jmmm.2019.166151
182. Y. Duan, X. Wen, B. Zhang, G. Ma, T. Wang, J. Magn. Magn. Mater. (2020). https://doi.org/10.1016/j.jmmm.2019.165947
183. C. Shang, E. Axinte, W. Ge, Z. Zhang, Y. Wang, Surf. Interfaces (2017). https://doi.org/10.1016/j.surfin.2017.06.012
184. J. Wang, Z. Zheng, X. Jing, Y. Wang, J. Magn. Magn. Mater. (2014). https://doi.org/10.1016/j.jmmm.2013.11.049
185. Z. Fu, B.E. MacDonald, A.D. Dupuy, X. Wang, T.C. Monson, Mater. Today (2019). https://doi.org/10.1016/j.apmt.2019.04.014
186. R.K. Mishra, J. Magn. Magn. Mater. (2019). https://doi.org/10.1016/j.jmmm.2019.03.129
187. R.K. Mishra, R.R. Shahi, J. Magn. Magn. Mater. (2017). https://doi.org/10.1016/j.jmmm.2017.06.124
188. K. Zaara, M. Chemingui, S. Le Gallet, Y. Gaillard, L. Escoda, J. Saurina, J.J. Suñol, F. Bernard, M. Khitouni, V. Optasanu, Crystals (2020). https://doi.org/10.3390/cryst10100929
189. A. Yakın, T. Şimşek, B. Avar, et al., Appl. Phys. A Mater. Sci. Process. (2022). https://doi.org/10.1007/s00339-022-05836-y
190. H. Kalantari, M. Zandrahimi, M. Adeli, H. Ebrahimifar, Intermetallics (2022). https://doi.org/10.1016/j.intermet.2022.107694
191. P. Kumari, R.K. Mishra, A.K. Gupta, S. Mohapatra, R.R. Shahi, J. Alloys Compd. (2023). https://doi.org/10.1016/j.jallcom.2022.167451
192. M. Panigrahi, B. Avar, J. Mater. Sci. Mater. Electron. (2021). https://doi.org/10.1007/s10854-021-06612-z
193. X. Jing, E. Axinte, Z. Zhao, Y. Wang, J. Magn. Magn. Mater. (2016). https://doi.org/10.1016/j.jmmm.2016.04.067

Authors and Affiliations

Alican Yakin[1] · Tuncay Simsek[2] · Baris Avar[3] · Telem Simsek[4] · Arun K. Chattopadhyay[5]

Alican Yakin
alican-mengel49@hotmail.com

Baris Avar
barisavar@beun.edu.tr

Telem Simsek
telem@nnthacettepe.com

Arun K. Chattopadhyay
akchatto@gmail.com

[1] Department of Industrial Design Engineering, Gazi University, Yenimahalle, 06500 Ankara, Turkey

[2] Department of Mechanical and Metal Technologies, Kırıkkale University, 71450 Kırıkkale, Turkey

[3] Department of Metallurgical and Materials Engineering, Zonguldak Bülent Ecevit University, 67100 Zonguldak, Turkey

[4] Department of Nanotechnology and Nanomedicine, Graduate School of Science and Engineering, Hacettepe University, Ankara, Turkey

[5] Uniformity Labs, Fremont, CA 94538, USA